CORA Cork Open Research Archive
Cartlann Taighde Oscailte Chorcaí

Title	Optimising transfection methods for genome editing using iPSCs and CRISPR/Cas9
Authors	Beltran, Jhoan Sebastian
Publication date	2026-02-28
Original Citation	Beltran Guiza, J. S. 2026. Optimising transfection methods for genome editing using iPSCs and CRISPR/Cas9. MRes Thesis, University College Cork.
Type of publication	Masters thesis (Research)
Rights	© 2026, Jhoan Beltran. - https://creativecommons.org/licenses/by-nc-nd/4.0/
Download date	2026-11-07 11:04:52
Item downloaded from	https://hdl.handle.net/10468/19302

UCC
University College Cork, Ireland
Coláiste na hOllscoile Corcaigh

University College Cork

School of Biochemistry and Cell Biology

Optimising transfection methods for genome editing using iPSCs and CRISPR/Cas9

Author: Jhoan Sebastian Beltran

Supervisor: Prof. Elena Matsa

Co-supervisor: Dr Ciaran Lee

February 2026

Author: Jhoan Sebastian Beltran

Supervisor: Prof. Elena Matsa

Co-supervisor: Prof. Ciaran Lee

A thesis submitted in partial fulfilment of the requirements for the degree of

Master of Research (MRes) in Biochemistry and Biosciences

University College Cork

Abstract

The emergence of induced pluripotent stem cells (iPSCs), together with major advances in genome editing technologies, has significantly expanded the potential of cell-based therapies in regenerative medicine and immunotherapy. Since their first description by Shinya Yamanaka and Kazutoshi Takahashi in 2006, iPSCs have been widely explored as a promising platform for the treatment of a broad range of diseases, including Parkinson's disease, Alzheimer's disease, and organ failure. Their capacity for unlimited self-renewal and differentiation into virtually any somatic cell type make them an attractive and versatile cell source for therapeutic applications.

Despite these advances, significant clinical challenges remain. One of the principal barriers to the clinical translation of iPSC-derived therapies is the potential immune rejection associated with allogeneic cell products. Consequently, multiple strategies have been proposed to mitigate immune recognition and improve the compatibility of transplanted cells.

This project aimed to contribute towards the development of hypoimmune iPSC lines by targeted knock-out of human leukocyte antigen (HLA) class I and class II molecules. To achieve this, the study evaluated alternative approaches for the delivery of genome editing cargo into iPSCs, assessing their potential as less invasive alternatives to electroporation. Transfection efficiencies obtained through cell-penetrating peptide (CPP)-mediated delivery and Lipofectamine-based methods reached approximately 40–50%%, with CPPs allowing higher viability and preservation of cellular morphology. In contrast, photoporation yielded lower transfection efficiencies, averaging around 22%. Overall, these findings suggest that CPPs may provide improved balance between cargo uptake and viability for iPSCs and will support future efforts to generate hypoimmune cell lines research and therapeutic applications.

Table of Contents

Abstract 3

Declaration 7

1. Introduction 8

2. Literature Review 14

2.1 Molecular Foundation of iPSCs and Applications in Disease Modelling and Research 14

2.2 Genome Editing methods and mechanisms 19

2.3 Hypoimmune Cell Production 27

2.4 Cellular delivery methods for genome editing components 30

3. Materials and Methodology 33

3.1 Cell Maintenance and Expansion 33

3.2 Cell Counting and Viability 34

3.3 Cell Bank Preparation and Storage 35

3.4 Cellular Transfection 36

3.4.1 Cellular transfection driven by cationic lipids 36

3.4.2 Cellular transfection driven by Cell Penetrating Peptides 38

3.4.3 Cellular transfection driven by photoporation 39

3.5 HPRT, B2M and CIITA knockout 40

3.6 crRNA off-target binding analysis 40

3.7 Genomic DNA extraction 41

3.8 DNA quantification 41

3.9 PCR primer design 41

3.10 Polymerase chain reaction (PCR) 42

3.11 PCR product purification and Sanger sequencing 43

3.12 Image processing 44

3.13 Statistical analysis 46

3.14 Illustrations 46

4. Results 47

4.1 iPSC culture and banking 47
4.2 Optimisation of enzymatic passaging time 47
4.3 Optimisation of coating reagent 49
4.4 Optimisation of DNA extraction from iPSC 49
4.6 Optimisation of PCR amplification with HPRT, B2M, and CIITA custom primers 57
4.7 Lipofection of B2M and CIITA gRNAs into iPSC for gene knock-out 58
4.8 Cargo delivery to iPSC *via* photoporation 62
4.9 Cargo delivery to iPSC via Cell Penetrating Peptides (CPPs) 65

5. Discussion 69

6. Acknowledgements 77

7. Bibliography 78

Table of Figures

Figure 1. Overview of autologous versus allogeneic iPSC-derived cell therapies..... 11
Figure 2.Summary of Project Stages. 13
Figure 3. Schematic representation of Yamanaka factors and their cellular effects during somatic cell reprogramming. 16
Figure 4. Schematic of CRISPR/Cas9 tools for genome and epigenome editing. 24
Figure 5. Cell images processing..... 45
Figure 6. SCTi003-A Cell Line Culture Optimization. 48
Figure 7. DNA extraction using three different methods. 51
Figure 8. Transfection condition optimisation. 54
Figure 9. Transfection using the L1R3 condition. 57
Figure 10. HPRT, B2M and CIITA knock-outs. 61
Figure 11. PCR-Cleaning and Sanger sequencing results. 62
Figure 12. Photoporation of FITC-Dextran nanoparticles into iPSC. 65
Figure 13. Transfection-mediated via cell-penetrating peptides. 69

Declaration

This is to certify that the work I am submitting is my own and has not been submitted for another degree, either at University College Cork or elsewhere. All external references and sources are clearly acknowledged and identified within the contents. I have read and understood the regulations of University College Cork concerning plagiarism and intellectual property.

Digital Signature of the candidate:

Jhoan S. Beltran

1. Introduction

The past has shaped our current society; in science, previous discoveries and experiments have led to the development of new theories and inventions. These discoveries have brought researchers closer to finding more effective treatments for diseases that affect people today. We could say that the early history of stem cell biology was influenced by James A. Till and Ernest A. McCulloch, who made one of the first observations pointing to the existence of an undifferentiated cell in hematopoietic tissue while investigating the sensitivity of radiation in mammalian cells (Till & McCulloch, 1961). Almost thirty-five years after Till and McCulloch's observations, at the Wisconsin Primate Research Centre, the American biologist James Thomson was isolating the first non-human primate embryonic stem cells while, simultaneously, Keith Campbell and his colleagues announced the Dolly sheep cloning by modifying the embryo of a sheep, marking a new era not just for cloning or developmental biology, but also for stem cell research (Campbell et al., 1996; McGraw et al., 2024; Thomson et al., 1998).

Such experiments provided evidence that undifferentiated cells could be used in multiple ways, including being manipulated to produce a cloned organism. However, cells with unlimited self-renewal capacity and the potential to differentiate into cell types derived from the three germ layers were thought to exist only in embryos. This changed in the summer of 2006, when an article published in *Cell* described a method to dedifferentiate somatic cells to generate pluripotent stem cells (Takahashi & Yamanaka, 2006) by forcing the expression of four genes: octamer binding transcription factor 4 (OCT4), Krüppel-like factor 4 (KLF4), sex-determining region Y-box 2 (SOX2), and c-Myc (OSKM); in an embryonic stem cell-like environment. Yamanaka and Takashi found a way to create what they called induced pluripotent stem cells (iPSCs), demonstrating that embryonic-like cells could be produced from somatic cells; their research established a new way to derive pluripotent cell types without the ethical implications of destroying an embryo.

Yamanaka and Takahashi's discovery gave rise to a better understanding of the molecular mechanisms controlling cellular differentiation and was subsequently replicated using human fibroblasts (Takahashi et al., 2007). Interestingly, almost at the same time, Jamie Thomson was publishing an alternative method to produce iPSCs using the previously described reprogramming factors *OCT4* and *SOX2* by Yamanaka, but adding *NANOG* and *LIN28*, instead of the proto-oncogenes *C-MYC* and *KLF4* (J. Yu et al., 2007), achieving a pluripotent state by using different transcription factors. Later experiments would demonstrate that it was possible not only to use different reprogramming factors but also a variety of delivery methods to introduce dedifferentiation signals into somatic cells to produce iPSCs (Doss & Sachinidis, 2019; Poetsch et al., 2022; Shi et al., 2024).

Since then, the production of iPSCs has been scaled up to enable their research in tissue repair or immune system modulation. Depending on the cell donor, the therapy can be classified as either autologous, where a patient's own cells are used to generate iPSCs, or allogeneic, in which donor cells are reprogrammed into iPSCs (Figure 1). Since 2018, pluripotent stem cell–derived therapies have transitioned from ESCs to iPSCs, and specifically into allogeneic iPSC therapies, which have been reported as the most common type of iPSC-based cell therapy over autologous (Kim et al., 2022) and the most frequently used cell source in iPSC-related clinical trials (Kirkeby et al., 2025). This trend partly reflects the need for pluripotent stem cell–derived products that can be readily available for patients requiring tissue repair (regenerative medicine) or enhanced immune response to treat cancer or other conditions (immunotherapy).

In regenerative medicine, iPSCs have been investigated for their ability to generate specialised tissues that can be used to treat degenerative disorders where cellular viability is affected. Sickle Cell Disease, Fanconi anaemia (Aboul-Soud et al., 2021), Parkinson's disease or Alzheimer's disease (Doss & Sachinidis, 2019; Fang et al., 2022; Shi et al., 2024)

are just some examples. Consequently, iPSCs have become promising candidates for the treatment of disorders in which tissue replacement may improve patients' quality of life.

Production of immune cell types from iPSC has allowed them to be used in immunotherapies (Chavez et al., 2025; Lim & June, 2017). For instance, iPSC-derived cell products with a chimeric antigen receptor (CAR) genetically modified have been shown to enhance the recognition of specific antigens with higher affinity (Chang et al., 2018), a feature that can be relevant to improve cancer cells recognition. The CD19-targeted CAR-NK candidate FT596 (Fate Therapeutics, Inc., 2021) is a good illustration of CAR therapies used in cancer can achieve objective responses in relapsed/refractory B-cell lymphoma patients in early-phase testing, including in patients who had previously failed autologous CAR-T therapy, without dose-limiting toxicities or observed cases of graft vs. host disease (GvHD). Similarly, iPSC-derived CD19 CAR-T candidate FT819 has demonstrated meaningful and durable responses in autoimmune conditions such as systemic lupus erythematosus and systemic sclerosis (Fate Therapeutics, Inc., 2021)

Depending on the cell source, iPSC-derived therapies can be classified as either autologous, where a patient's own cells are used to generate iPSCs, or allogeneic, in which donor cells are dedifferentiated into iPSCs (Figure 1). Since 2018, pluripotent stem cell–derived therapies have transitioned from ESCs to iPSCs, with allogeneic iPSCs becoming the most frequently used cell source in clinical trials by 2025 (Kim *et al*. 2022; Kirkeby et al., 2025). This trend partly reflects the need for pluripotent stem cell–derived products that can be produced rapidly and be readily available for patients requiring urgent treatment. Hypoimmune allogeneic iPSC-based therapies meet these requirements, and will be discussed in more detail in section 2.3 of this thesis.

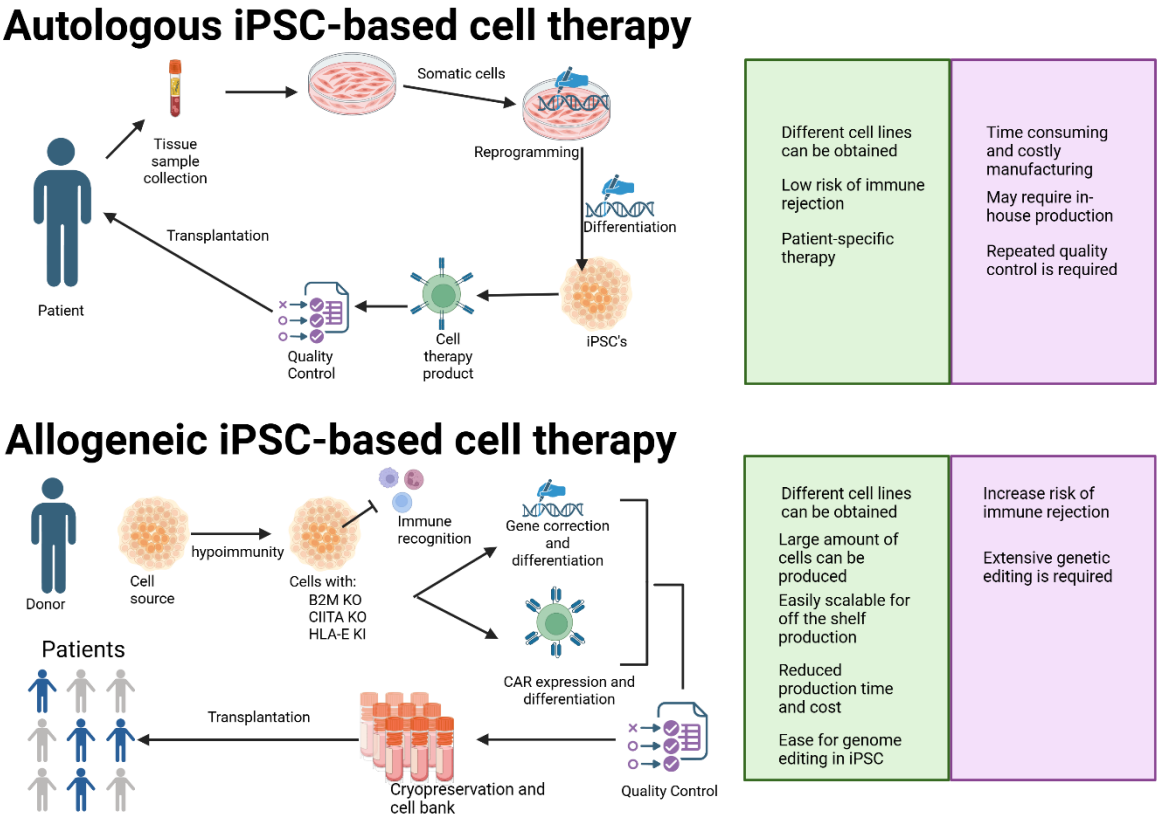

Figure 1. Overview of autologous versus allogeneic iPSC-derived cell therapies.

Autologous therapies reprogram and differentiate patient cells for re-transplantation, minimising immune rejection but requiring individualised, time-consuming manufacturing. Allogeneic therapies use gene-edited donor iPSC lines to create banked "off-the-shelf" products for multiple patients, enabling scalability but increasing immunological and genetic-editing challenges.

Induced pluripotent stem cells (iPSCs) can generate a wide variety of cell products that can be expanded and/or modified to treat degenerative diseases or enhance immune responses. Despite significant advances, several critical factors must be addressed to ensure the safety, efficacy, and reproducibility of iPSC-derived therapies. One major factor is the method used to deliver transcription factors during reprogramming, which can be either integrative or non-integrative. Integrative methods, such as PiggyBac transposons or retroviral and lentiviral vectors, offer high efficiency but carry risks of insertional mutagenesis. Non-integrative

approaches, including Sendai virus (an RNA, episomal virus), episomal plasmids, minicircle DNA vectors, synthetic mRNA, and protein-based delivery, reduce genomic risk but often show lower efficiency (Poetsch et al., 2022; Zakrzewski et al., 2019). Optimising these delivery methods to maximise efficiency while minimising toxicity and genomic alterations remains a key priority in iPSC research.

Even when high-quality iPSC-derived cells are produced, transplantation presents additional challenges, especially for allogeneic cell therapies. These include the potential for teratoma or tumour formation, immune rejection (host-versus-graft disease), and graft-versus-host disease, all of which pose significant safety concerns (J. Han et al., 2024; Liang et al., 2015; Wang et al., 2022). To address the latter issue, several strategies have been proposed, including blocking the expression of key genes that regulate HLA class I and class II molecules, promoting the expression of immune-inhibitory signals, or introducing alternative HLA receptors, such as HLA-E, to evade immune detection. However, these approaches have demonstrated only partial immunomodulatory effects, highlighting the need for further investigation to advance iPSC-based therapies and achieve an optimal balance between immune evasion and immune control (Murugan et al., 2022).

This project aimed to develop and optimize conditions for generating hypoimmune iPSCs lacking HLA class I and II through CRISPR/Cas9 genome editing delivered via lipid-based and alternative transfection systems. To support this goal, cell culture conditions for the SCTi-003-A cell line were optimized by evaluating parameters such as cell growth, morphology, seeding density, trypsin exposure time, and the use of recombinant proteins and animal-derived matrix coatings. In parallel, molecular workflows including DNA extraction, PCR amplification of key genes, and Sanger sequencing were refined to ensure downstream analysis. Furthermore, three transfection methods were compared: lipofection, photoporation, and CPP-mediated delivery to assess transfection efficiency and cell viability to establish optimal conditions for cargo delivery that can be used in future research (Figure 2).

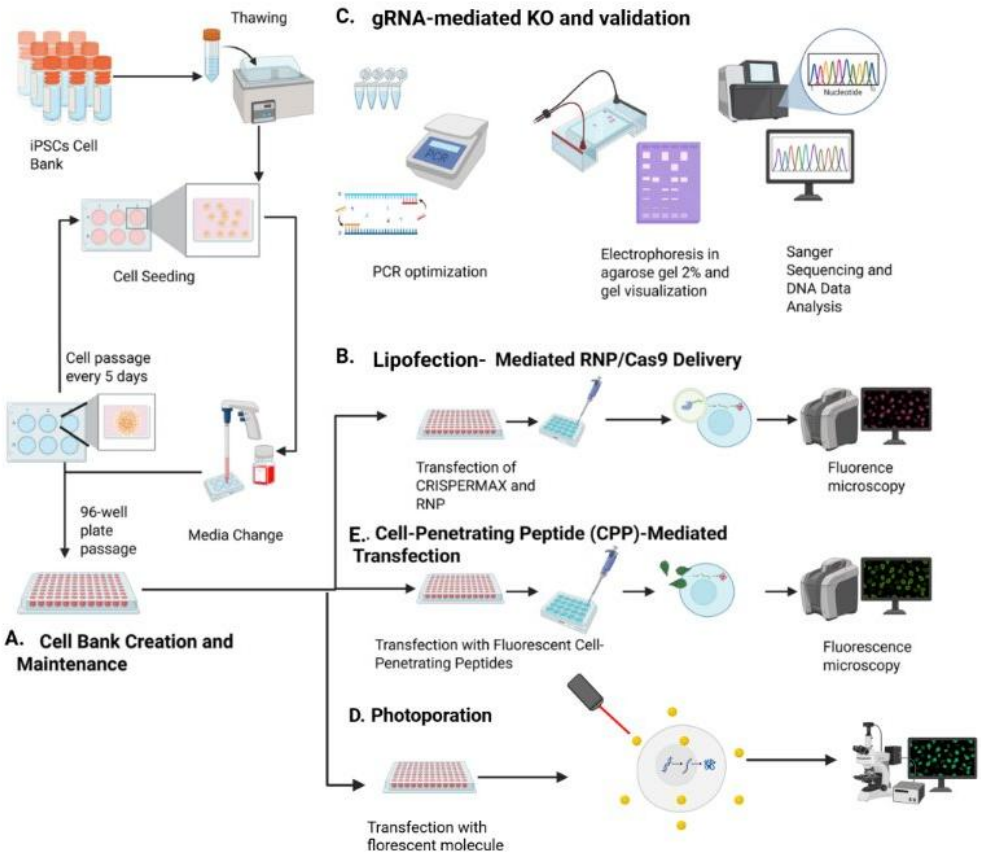

Figure 2.Summary of Project Stages.

Project organization was divided into five stages: (A) optimization of cell culture conditions for the iPSC cell line SCTi-003-A, including cell seeding density, trypsin exposure time, passaging frequency, coating reagent selection, and cell banking; (B) knockout of genes associated with HLA class I and II using the CRISPR/Cas9 system delivered via lipofectamine, with fluorescent crRNA included to assess cell viability; (C) evaluation of transfection outcomes from stage B using Sanger sequencing; and (D–E) comparison of two additional transfection methods for iPSCs, photoporation and CPP-mediated transfection, in terms of efficiency and cell viability.

2. Literature Review

Induced pluripotent stem cells (iPSCs) play a crucial role in stem cell research. Since their discovery in 2006 by Takahashi and Yamanaka, iPSCs have been the focus of extensive investigation worldwide. These cells are characterized by a high capacity for self-renewal and pluripotency, which enables them to differentiate into virtually any cell type in the human body. This review highlights some of the most significant features of iPSCs and is structured into three sections that support the main objective of this thesis. First, we discuss the molecular foundations of iPSCs, including pluripotency, differentiation potential, and the challenges associated with their use in cell-based therapies. Next, we examine genome editing in iPSCs and the mechanisms currently employed, providing an overview of state-of-the-art technologies and strategies to confer hypoimmunity in iPSCs. Finally, we address the current approaches for generating hypoimmune iPSCs, and discuss their importance.

2.1 Molecular Foundation of iPSCs and Applications in Disease Modelling and Research

iPSCs are defined by their self- renewal capacity and differentiation potential, features that allow them to generate any cell type in the human body (Y. Chen et al., 2024). In 2006, Shinya Yamanaka described a method to generate iPSCs using four transcription factors (Takahashi & Yamanaka, 2006). These factors: Oct3/4, Sox2, c-Myc, and Klf4 (OSKM), were introduced into fibroblasts *via* retroviral particles as a transduction mechanism to revert differentiated cells to a pluripotent state. Subsequent studies demonstrated that pluripotency could also be achieved using alternative genes and delivery methods, including adenoviruses,

Sendai Virus (SeV), mRNA/microRNA, or episomal plasmids (Aboul-Soud et al., 2021; Wang et al., 2022; J. Yu et al., 2007).

OSKM transcription factors interact with chromatin, leading to a widespread loss of accessibility at somatic gene regions while promoting increased accessibility at loci associated with pluripotency (Figure 3) (Park et al., 2024). Consequently, the four factors induce pluripotency by driving extensive remodelling of the transcriptome and epigenome, including changes in DNA methylation, histone acetylation, and ATP-dependent chromatin remodelling Specifically, C-MYC promotes chromatin opening by interacting with methylated regions and facilitating a more accessible chromatin state (Aboul-Soud et al., 2021; Wang et al., 2022; J. Yu et al., 2007).

These molecular changes are accompanied by marked morphological alterations, such as those observed during the reprogramming of fibroblasts into iPSCs, a process that involves a mesenchymal-to-epithelial transition (MET). This transition is driven by mechanisms including Oct3/4-mediated repression of epithelial-to-mesenchymal transition (EMT) drivers such as Snail and TGF-β signalling and activation of ectodermal genes, as well as Klf4-induced upregulation of epithelial markers such as E-cadherin (Cdh1) (Y. Chen et al., 2024). Moreover, OCT3/4 and SOX2 directly regulate genes associated with somatic cell identity as well as pluripotency-associated genes, and activate additional factors, such as NANOG, FGF4, and osteopontin, which, together with KLF4, contribute to the establishment and maintenance of pluripotency (Park et al., 2024).

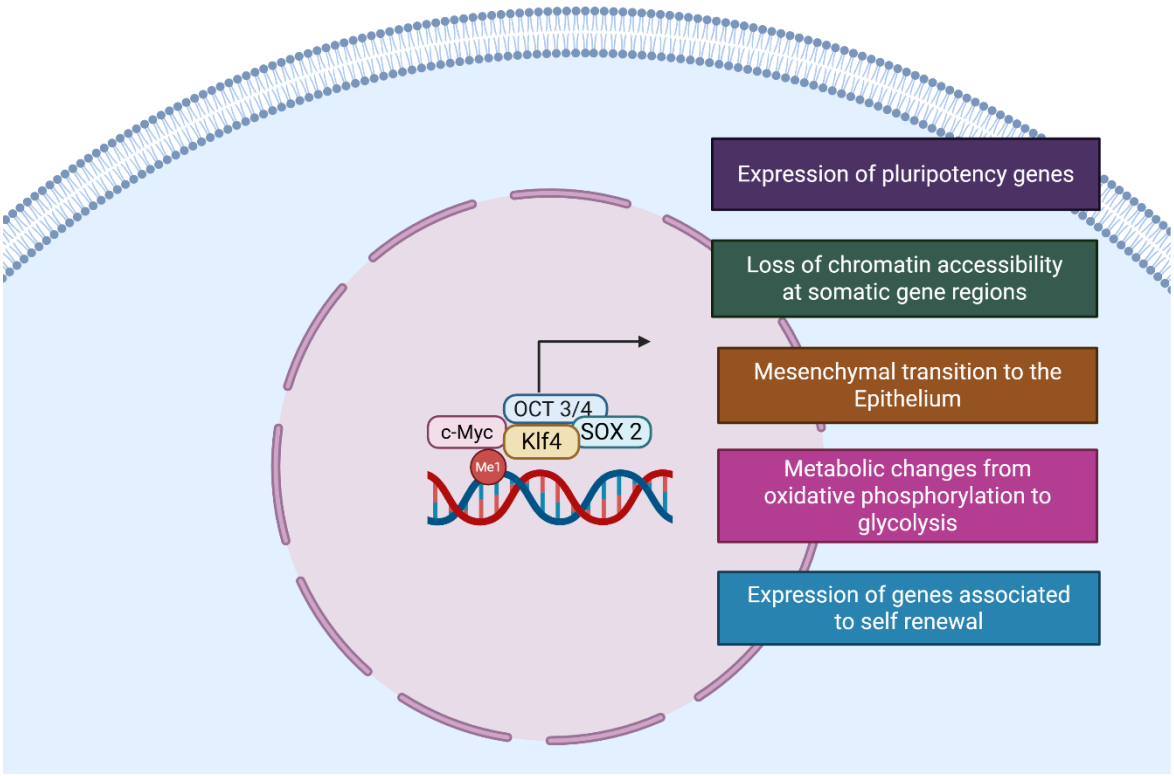

Figure 3. Schematic representation of Yamanaka factors and their cellular effects during somatic cell reprogramming.

The Yamanaka factors OCT3/4, SOX2, KLF4 and c-MYC act on somatic chromatin to induce pluripotency, leading to (i) activation of pluripotency and self-renewal gene networks, (ii) loss of chromatin accessibility at somatic gene regions, (iii) a mesenchymal-to-epithelial transition, and (iv) a metabolic shift from oxidative phosphorylation to glycolysis.

The four genes identified by Yamanaka and Takahashi represent the gold standard for reprogramming somatic cells into induced pluripotent stem cells (iPSCs). However, KLF4 and C-MYC exhibit oncogenic properties, as their integration into the genome can promote uncontrolled proliferation and tumorigenesis (Inagaki, 2023; Luo et al., 2025). In particular, C-MYC functions as a transcription factor that regulates genes involved in cell proliferation,

and its deregulation through inhibition of cell cycle checkpoints has been linked to DNA double-strand breaks (DSBs), chromosomal structural alterations, impaired DNA repair mechanisms, and increased reactive oxygen species production (Aguirre et al., 2023; Dhanasekaran et al., 2022). Together, these oncogenic properties underscore the need to carefully consider the role of C-MYC in reprogramming, while also highlighting the importance of examining how other pluripotency-associated transcription factors contribute to genomic stability and self-renewal (Fiorini et al., 2025; Gao et al., 2023; Kress et al., 2015). Accordingly, some studies have demonstrated that KLF4 and C-MYC can be replaced by alternative factors, such as NANOG and LIN28, achieving comparable reprogramming efficiency and cell fate reversion without reliance on C-MYC (Aguirre et al., 2023; Park et al., 2024)

The risk of tumorigenesis is not limited to the deregulation of C-MYC; other transcription factors, such as SOX2, can also acquire mutations that contribute to malignant transformation. SOX2 is a key regulator of pluripotency and is essential for the reprogramming and generation of iPSCs (An et al., 2019). However, when mutated, SOX2 can promote anti-apoptotic signalling and autophagy, and through interaction with β-catenin, regulate ABCC2, ultimately driving the conversion of normal cells into a malignant phenotype and promoting tumour progression (Zhu et al., 2021). Since the introduction of the OSKM factors, alternative reprogramming strategies have been proposed to produce safer iPSCs. In 2022, Deng et al. reported the generation of the first chemically induced pluripotent stem cells (CiPSCs), designed to reduce the risk associated with oncogene integration (Guan et al., 2022). Reprogramming efficiency has also been enhanced through the use of epigenetic modulators, such as DNA methyltransferase inhibitors, histone deacetylase inhibitors, and the histone methylation regulator Neplanocin A (DZNep), which have been shown to improve the robustness of the reprogramming process (Takahashi & Yamanaka, 2016).

These discoveries have enabled the use of iPSCs to model degenerative diseases such as Parkinson's disease, cardiac injury, and Duchenne muscular dystrophy (DMD). Among these, DMD has been extensively studied, as iPSCs can be differentiated into cardiomyocytes and myoblasts, cell types that are primarily affected in this disorder. These models faithfully recapitulate the human disease phenotype, highlighting the potential of human iPSC-based approaches. Specifically, iPSC derivatives from DMD patients demonstrate dystrophin loss, abnormal calcium handling, mitochondrial dysfunction, increased ROS, dysregulated iron metabolism and altered electrophysiology, similar to patients diagnosed with DMD, supporting their value for drug discovery and disease modelling. Due to this molecular and phenotypical similarity, iPSC-derived organoids have also shown particular promise for modelling DMD-associated cardiac manifestations, such as myocardial infarction and hypertrophic cardiomyopathy (Choi et al., 2021; Moriyama & Yokota, 2025; Przymuszała et al., 2026).

In the case of cancer, which is associated with over ten million deaths every year worldwide, iPSCs can be used to understand cancer initiation and progression, therapeutic vaccine development, and generation of immune cell types for cell immunotherapy (P. Chen et al., 2025). Thanks to their indefinite self-renewal capacity and pluripotency, iPSCs are useful for producing immune cells such as NK and T cells, which have been particularly important in cancer treatment. NK and T cells can be generated from iPSCs, enabling scalable production of iPSC-derived NK or T cells that can subsequently be genetically modified, as they are relatively easy to edit, and immune cells derived from iPSCs can be efficiently engineered, representing a major advantage for the development of allogeneic "off-the-shelf" immunotherapy products (Zhang et al., 2025). This approach helps evade allogeneic immune rejection and reduces the risk of graft-versus-host disease (GvHD). Additionally, iPSC-derived NK cells have shown homogeneous and highly standardized cell products that can be scaled up for clinical use (Alali et al., 2025). These cells have been used to generate iPSC-derived CAR-NK cells capable of recognizing specific tumor-associated antigens, such as CD276 in human esophageal squamous cell carcinoma and MUC1 in human tongue squamous cell carcinoma. In the case of T cells, and specifically CAR-T autologous cell

therapy, which commonly presents manufacturing delays, high production costs, and standardization challenges, iPSCs could be used to generate T cells (CAR-iT) and enable the production of allogeneic CAR-T therapies that can be scaled up and avoid immune rejection. Thus, immune cell therapies can also benefit from iPSCs, as they provide a platform for the scalable and standardized production of engineered immune cells (P. Chen et al., 2025; Mishra & Kalyuzhny, 2024).

2.2 Genome Editing methods and mechanisms

Genome editing is a method by which DNA can be modified to change the nucleotide sequence through deletion, insertion, or substitution of genetic material. Since the discovery of restriction enzymes in the 1960s, researchers have been able to modify genetic information, using different methods. One of the first approaches developed to create DNA double-strand breaks was zinc finger nucleases (ZFNs), engineered nucleases that combine a zinc finger DNA-binding domain with a FokI nuclease cleavage domain (Gaj et al., 2012). The same FokI nuclease was later used to develop transcription activator-like effector nucleases (TALENs), considered a next generation of ZFNs and introduced around 2010–2011. Both technologies enable targeted DNA breaks to facilitate genome editing (Kwon et al., 2021).

However, these tools were difficult and time-consuming to target specific genomic regions. ZFN and TALENS, were often expensive and technically demanding (Saha et al., 2019). In 2012, with the discovery of CRISPR/Cas9 as a more accessible and versatile alternative, costs and time were reduced, and genome editing became easier to achieve. Since its introduction, multiple modified versions of Cas9 have been developed to improve targeting accuracy, generate single-strand breaks, and reduce associated risks, thereby enhancing

genome editing strategies (G. Liu et al., 2020; Modell et al., 2022; Ramirez-Phillips & Liu, 2021). This section focuses on these genome editing techniques, describing the basic principles of ZFNs and TALENs, with particular emphasis on CRISPR/Cas-based approaches and its various modifications.

In 1996, zinc finger nucleases (ZFNs) were developed for genome editing. These synthetic enzymes are composed of the fusion of FokI, a type IIS restriction endonuclease originally identified in *Flavobacterium okeanokoites* (El Semary et al., 2026), with a sequence-specific DNA-binding zinc finger domain. When FokI recognises the sequence 5′-GGATG-3′, it dimerizes with another FokI nuclease monomer bound to the complementary strand and cleaves the DNA, creating a double-strand break (DSB) (Ingle et al., 2025). Through the incorporation of pre-customised zinc finger proteins, researchers were able to target specific genomic sites to generate DSBs. Each zinc finger protein forms a three-dimensional structure stabilized by a zinc ion and recognises a triplet of nucleotides. By combining multiple zinc finger repeats, it is possible to target a wide range of DNA sequences within the genome. Despite their declining use due to the labour-intensive methods required to synthesise zinc finger proteins specific for individual nucleotide triplets, ZFNs played a pivotal role in the development of genome editing technologies. Notably, ZFNs enabled the first gene-editing-based therapeutic approach against HIV (SB-728) to advance to clinical trials and laid the foundation for many of the genome engineering methods available today (Chadwick & Musunuru, 2017; D. Liu et al., 2025).

Following the development of ZFNs, an alternative, known as transcription activator-like effector nucleases (TALENs), was introduced in 2010 (Christian et al., 2010). Early applications of this technology successfully generated knockouts in rats and mice. TALENs were easier to produce because, unlike ZFNs, which often required external design companies, TALENs could be developed locally using plasmids that could be assembled through a convenient Golden Gate cloning protocol (Bisht et al., 2024). ZFNs and TALENs

share the same FokI nuclease; however, instead of ZFNs, TALENs combine FokI with TAL effector proteins, originally secreted by Xanthomonas species to manipulate host plant gene expression during infection (Kwon et al., 2021). These TAL proteins determine the specificity of the system through repeat variable di-residues (RVDs), which recognize individual nucleotides. This feature improved on ZFNs, whose zinc finger proteins recognize nucleotide triplets, allowing TALENs to achieve higher specificity. As a result, TALENs generate double-strand breaks (DSBs) after recognition of the target sequence and dimerization of the nuclease, offering higher accuracy, greater efficiency, and lower off-target rates compared to ZFNs. This technology has been applied in gene therapy approaches involving induced pluripotent stem cells (iPSCs) in preclinical studies (Bisht et al., 2024). Despite its advantages over ZFNs, TALENs required laborious engineering, customisation, and lengthy validation processes. These limitations contributed to the rapid adoption of the CRISPR/Cas9 system, developed in 2012, which allowed genome editing in a wider range of organisms thanks to its versatility and ease of use (Liu et al., 2025).

In 2012, CRISPR/Cas9 was introduced as an efficient genome-editing method capable of targeting specific DNA sequences with exceptional design adaptability. Since then, it has become one of the most widely used tools for genome editing. Earlier foundational studies on genome editing using ZFNs and TALENs highlighted the labour-intensive processes, high costs, and complex engineering required to generate zinc-finger and TAL proteins. Moreover, the protein–DNA Watson–Crick interactions underlying these methods were shown to be biochemically less stable than the base-pairing interactions created by CRISPR/Cas9, which in part explain the widespread adoption of this newer technology over earlier methods (Adli, 2018; Freitas-Alves et al., 2025; Modell et al., 2022).

The SpCas9 multifunctional enzyme has 1,368 amino acid residues and is composed of the alpha helical-recognition REC lobe and the nuclease NUC lobe, which contains the conserved HNH and RuvC nuclease domains (Freitas-Alves et al., 2025). The enzyme was

first identified in *Streptococcus pyogenes* as part of an adaptive immune system against bacteriophage infections (Chadwick & Musunuru, 2017). The mechanisms to edit a genome using the CRISPR/Cas9 system require two basic components: i) the Cas 9 enzyme and ii) a small RNA molecule responsible for paring at the specific site, which can be a single molecule known as single guide RNA (sgRNA) or divided into two molecules: crispr RNA (crRNA), directing Cas9 to specific complementary DNA sequences for cleavage, and trans-activating CRISPR RNA (tracrRNA), responsible for joining the Cas9 and the crRNA (Bisht et al., 2024; Czerwińska et al., 2019; Kantor et al., 2020). Once Cas9 joins the RNA to form the ribonucleoprotein (RNP) complex, it can be directed to a specific DNA sequence and generate a Double-Strand Break (DSB) after recognition of a Protospacer Adjacent Motif (PAM). The latter is a critical recognition DNA sequence 2-6 bp long, which in the case of Cas9 is 5'-NGG-3', where N is any purine or pyrimidine (Freitas-Alves et al., 2025; Ingle et al., 2025). The DSB can then be repaired by non-homologous end joining (NHEJ) cellular mechanisms to generate a knock-out of the sequence of interest, or repaired by homologous recombination (HR) and generate a knock-in if a homologous template sequence is provided (Cao et al., 2025).

The CRISPR/Cas9 system has become one of the most widely used tools for genome editing. This technology, which earned Emmanuelle Charpentier and Jennifer Doudna the Nobel Prize in Chemistry in 2020, has been successfully combined with iPSC technology to investigate Mendelian disorders (Heinel, 2020). For example, in the case of DMD, it has been possible to restore up to 99.9% of the DMD open reading frames through targeted editing. However, further research is required to reduce stochastic DNA damage, minimise off-target effects, and overcome limitations imposed by PAM sequence requirements (Modell et al., 2022; Yuan et al., 2018).

To date, several genome-editing toolkits have been developed based on the discovery by Doudna and Charpentier. Additional variations of CRISPR/Cas9 technologies can be broadly

divided into two main categories: i) small-scale genome modifications and ii) epigenetic regulation (Figure 3). Small-scale modifications include prime editing and base editing, whereas epigenetic regulation includes technologies such as CRISPRi (interference), CRISPRa (activation), and CRISPRs (silencing).

Prime editing is a modification of the original CRISPR/Cas9 system that enables precise nucleotide changes without generating double-strand breaks (DSBs) that can be highly toxic to cells, and allows programmable nucleotide substitutions (D. Liu et al., 2025). This engineered method composed of a fused enzyme between Cas9 HNH mutant (creates nickase, nCas9, enzyme) attached to a reverse transcriptase (RT), and a prime-editing guide RNA (pegRNA) is a modified version of the traditional single-guide RNA (sgRNA) used in the CRISPR/Cas9 system and consists of a primer-binding site (PBS) extension at the 3′ end, and a reverse-transcription template(RTT) carrying the desired edit (Bisht et al., 2024; D. Liu et al., 2025; Shen et al., 2024). Upon target recognition, nCas9 introduces a single-strand nick at the specified genomic region. Next, the PBS sequence within the pegRNA anneals to the 3′ end upstream of the nick and serves as a primer for reverse transcription. The reverse transcriptase then synthesises the edited DNA sequence complementary to the pegRNA template adjacent to the nick. Subsequently, the unedited 5′ DNA flap is excised, allowing the newly synthesized edited strand to be ligated into the genomic DNA. This technology enables precise insertions, deletions, and base substitutions encoded in the pegRNA template, without the need for an exogenous donor DNA sequence. At the same time, this technology also reduces the activation of DNA repair pathways that can increase the likelihood of insertion–deletion (indel) mutations (Brooks et al., 2023; Kantor et al., 2020). Prime editing has been explored as an alternative therapeutic strategy for genetic diseases, such as correcting mutations responsible for β-thalassemia. Nevertheless, a major limitation of this technique is its relatively low editing efficiency, which is even more pronounced in iPSCs (Habib et al., 2022). Despite the advantages prime editing approaches, these findings highlight the need to optimize prime-editing efficiency in iPSCs before broader research or clinical application.

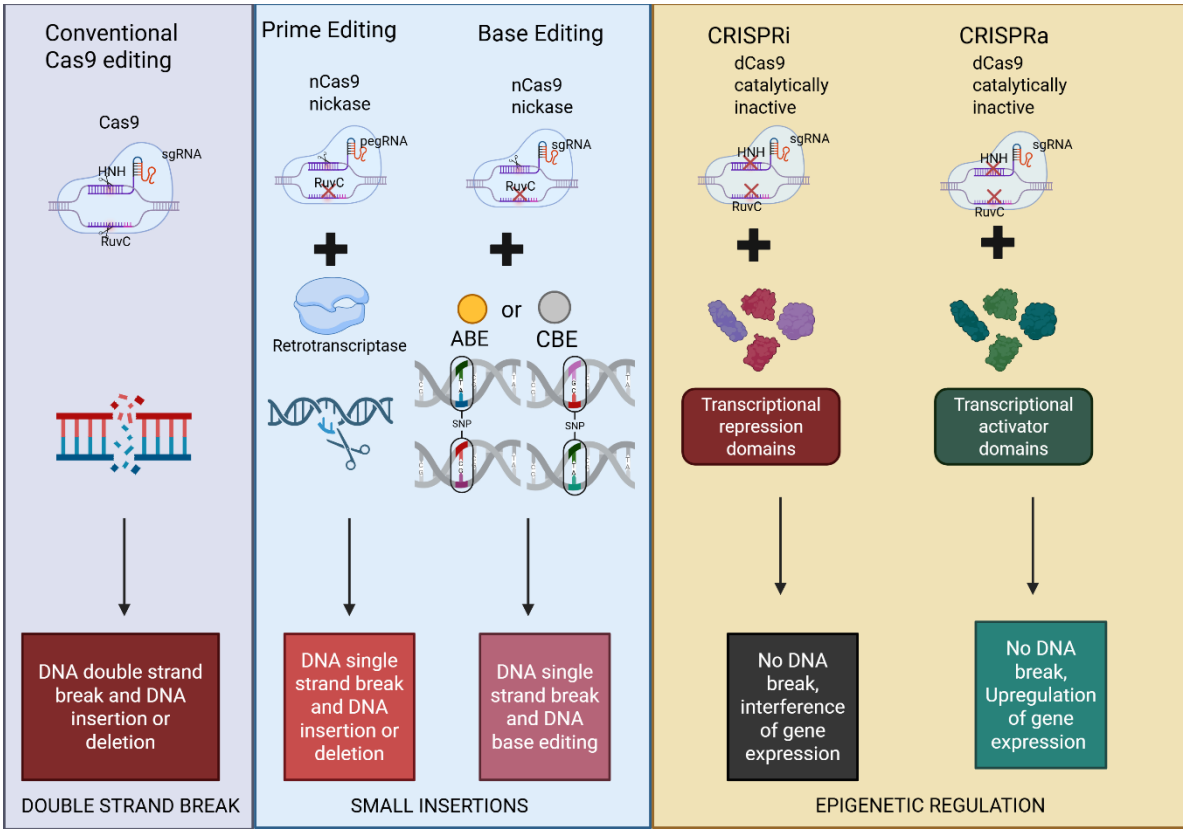

Figure 4. Schematic of CRISPR/Cas9 tools for genome and epigenome editing.

Conventional Cas9 introduces double-strand breaks that are repaired with insertions or deletions. Prime editing and base editing use Cas9 nickase (nCas9) fusions to install precise small insertions, deletions, or base substitutions without double-strand breaks. Dead Cas9 (dCas9) fusions enable regulation without sequence change: CRISPRi and CRISPRa inhibit or activate transcription.

Another method that complements the genomic editing tool kit is Base editing, a derivation technique from the CRISPR/Cas9 system that allows base change mutations. Two types of base editing have been developed: cytosine base editor (CBE) and adenine base editors (ABE). Both approaches typically combine a nickase Cas9 (nCas9) with a cytidine or adenine deaminase enzyme, a type of protein that controls the conversion of a base by removing an amino group, to catalyse the transition of C>T and A>G. The conversion from

C to T in CBE requires a temporary step from C to U, which activates the base excision repair (BER) DNA repair mechanism to synthesize a thymine in the uracil position. However, during that process, an intracellular uracil DNA glycosylase (UNG) can remove the uracil and restore the conversion to C:G making the genome editing less efficient. Thus, inhibitors of the UNG have been included and fused with the Cas 9 nickase enzyme such as uracil DNA glycosylase inhibitor (UGI)(Cao et al., 2025; Ingle et al., 2025). In the case of A> G, the process is similar. However, the deamination of adenine produces inosine, which DNA polymerases recognize as guanine causing a, A>G substitution during replication. Thus base editing is a powerful tool that could correct critical nucleotides in the human genome, promising novel avenues for future treatments (Koblan et al., 2021).

Beyond knock-out and knock-in base editing and prime editing, CRISPR-Cas9 technology has continued to evolve. It is now possible to modulate gene expression through epigenetic mechanisms, either activating (CRISPRa), silencing (CRISPRs) or inhibiting (interference) (CRISPRi) transcription (Shen et al., 2024). CRISPR/Cas9 technology use for epigenetic applications involves inactivating both Cas9 enzyme nuclease domains to generate a catalytically dead Cas9 (dCas9). dCas9 can be fused to transcriptional activation domains such as SAM, VPR, or SunTag to upregulate gene expression (CRISPRa). In addition, epigenomic modulators such as methyltransferases have been also fused with dCas9 to control the expression of a gene, which has been useful to target specific promoters in the genome(CRSIPRs) (Sung & Yim, 2020). Conversely, this modified enzyme can then be also fused with transcriptional repression domains, such as KRAB (e.g., KOX1-KRAB, KOX1-KRAB-MeCP2, or ZIM3-KRAB) to inhibit gene expression (CRISPRi) by interference with the promoter recognition (Adli, 2018).

More explicitly, CRISPR interference (CRISPRi) allows researchers to decrease the expression of both coding and non-coding RNAs by using a catalytically deactivated Cas9 (dCas9) fused to a transcriptional repressor domain, such as the Krüppel-associated box

(KRAB)(Cardiff et al., 2024). This dCas9-KRAB complex is guided to the target locus by a single-guide RNA (sgRNA) but is unable to generate double-strand breaks (Hu et al., 2024; Zhou et al., 2024). Once recruited to the promoter region, the complex induces repressive histone modifications, including histone methylation, through the recruitment of additional corepressor proteins, leading to chromatin compaction and transcriptional silencing (Cai et al., 2023).

In contrast, CRISPR activation (CRISPRa) promotes gene expression by fusing dCas9 to transcriptional activator domains, such as VP64. VP64 is a strong transactivation domain that recruits coactivators, including histone acetyltransferases (HATs) such as p300 (Cardiff et al., 2024; Shen et al., 2024). These interactions result in chromatin remodeling, increased chromatin accessibility, and enhanced recruitment of transcription factors, thereby activating gene transcription. CRISPR-based epigenetic regulation tools have been introduced relatively recently and have shown promising results in identifying key genes involved in cardiac development and disease (J. L. Han & Entcheva, 2023), both in *vitro* and *in vivo*, as well as in uncovering genes whose dysregulation contributes to disease pathology, particularly in multifactorial disorders (Bendixen et al., 2023; Razavi et al., 2024).

In summary, the evolution of CRISPR/Cas9 from basic genome editing to sophisticated epigenetic regulation has greatly expanded our ability to precisely control gene expression. These advances, together with complementary genome-editing tools such as TALENs and ZFNs, have enabled the creation of cellular models that not only help dissect disease mechanisms but also pave the way for therapeutic applications. In particular, combining the CRISPR/Cas9 and iPSCs technologies allows for the generation of engineered cell products with tailored genetic and epigenetic profiles. This includes the development of hypoimmune cells, which are modified to evade immune detection in allogeneic cell therapy settings, highlighting the potential of genome-editing technologies to enhance therapies for cancer, inherited disorders, and other diseases with unmet medical needs.

2.3 Hypoimmune Cell Production

iPSC and genome editing technologies have advanced research and development of new cell therapies for a variety of conditions, particularly for allogeneic iPSC-based products. It has been suggested that this type of cell therapy can reduce both costs and production time (Chen et al., 2025). However, one of the major challenges that still persists in the clinical application when it comes to allogeneic-based cell therapies is the elicited immune response, which can generate graft-versus-host disease (GvHD) and host-cell-mediated allorejection (Li et al., 2025). In the context of allogeneic transplantation, donor-derived cells can be recognised as foreign by the recipient's immune system, triggering immune responses that compromise therapeutic efficacy and patient safety. Over the years, various strategies have been proposed to overcome these immune barriers. Some approaches aim to knock down/out endogenous T-cell receptors (TCRs), replacing them with non-HLA-dependent chimeric antigen receptors (CARs) in T or NK cells, or express non-polymorphic HLA molecules such as HLA-E or HLA-G at the same time as knocking down/out polymorphic HLA-A, B, and C molecules (Hong et al., 2025). The goal of all these strategies is to develop hypoimmune engineered cells designed to evade immune recognition while maintaining their therapeutic functionality.

As introduced above, a central target in the development of hypoimmune cells is the modulation of the HLA system, which plays a fundamental role in immune surveillance and self–non-self-discrimination (Guney et al., 2026). The HLA system represents the human version of the major histocompatibility complex (MHC) and is encoded by a cluster of highly polymorphic genes located on chromosome 6 (6p21). This genomic region contains multiple loci that encode cell-surface glycoproteins responsible for presenting antigenic peptides to immune cells, thereby coordinating adaptive immune responses. Structurally, HLA class I molecules (including HLA-A, HLA-B, and HLA-C) are heterodimeric proteins composed of a polymorphic heavy α-chain associated with β2-microglobulin (B2M). The heavy chain contains three extracellular domains (α1, α2, and α3), where the α1 and α2 domains form the

peptide-binding groove that accommodates short intracellular peptides, typically 8–10 amino acids in length (Damian, 2026; Dolenc, 2025). These peptides are derived from proteins processed in the cytoplasm and transported into the endoplasmic reticulum by the transporter associated with antigen processing (TAP). Once loaded, the peptide–HLA complex is expressed on the cell surface and recognized by $CD8^+$ cytotoxic T lymphocytes, allowing the immune system to detect virus-infected or malignant cells (Dolenc, 2025).

In contrast, HLA class II molecules (primarily HLA-DR, HLA-DQ, and HLA-DP) are composed of two polymorphic chains (α and β), both of which contribute to the peptide-binding groove. These molecules are mainly expressed on professional antigen-presenting cells such as dendritic cells, macrophages, and B cells. HLA class II molecules present peptides derived from extracellular proteins that have been internalized and processed within endosomal compartments (Guney et al., 2026). The resulting peptide HLA complexes are recognized by $CD4^+$ helper T cells, which coordinate downstream immune responses, including cytokine production and activation of other immune cells.

Advances in genome editing technologies have provided powerful tools to modify genes involved in immune recognition pathways (Arrieta-Bolaños, 2025). In particular, the development of the CRISPR/Cas9 system has enabled precise and efficient genetic modifications in pluripotent stem cells. These technologies allow researchers to selectively disrupt or regulate genes to generate hypoimmune cells (Chaaithanya & Rajalingam, 2025). Specifically, knocking out molecules associated with MHC class I and II expression has emerged as a foundational strategy for creating "universal donor" stem cells. The knockout of B2M, which encodes beta-2 macroglobulin , has been used to overcome immune rejection mediated by $CD8^+$ in allogeneic cells (Bogomiakova et al., 2024). While disruption of B2M can minimize immunogenicity by evading $CD8^+$ T cells, it is insufficient to fully ensure transplant safety. Studies have shown that combining the disruption of B2M with other genes involved in MHC expression, such as CIITA, which is essential for MHC class II transcription, can generate more robust hypoimmune cells. In iPSC research, cells lacking both HLA class I and II have been successfully generated and differentiated into multiple

cell types, such as cardiomyocytes (Mattapally et al., 2018). This double knockout reduces T cell recognition and influences antigen presentation, raising potential concerns if allograft cells become infected or malignant. Such concerns are mitigated by introducing suicide genes (e.g., iCasp9 and HSV-TK/ganciclovir systems) into hypoimmune iPSCs developed for allogeneic therapeutic use (Khan et al., 2019; Kimura et al., 2019; Lipus et al., 2020).

Complete disruption of MHC can, additionally, trigger immune responses through the "missing-self" mechanism of natural killer (NK) cells (Hong et al., 2025; Li et al., 2025). Cells lacking HLA class I molecules may become targets for NK cells, which detect and eliminate cells exhibiting abnormal or missing self-antigens. Strategies combining the knockout of B2M and CIITA with NK cell inhibitory mechanisms have been developed to generate hypoimmune cells capable of evading both T cell and NK cell–mediated immune responses. NK cells detect the absence of self-MHC molecules *via* activating and inhibitory receptors. Specifically, inhibitory receptors such as CD94/NKG2A, NKG2B, and NKG2C recognize HLA-E, while killer cell immunoglobulin-like receptors (KIRs) interact with HLA-C, transmitting inhibitory signals that suppress NK cell cytotoxicity. To restore these inhibitory signals in hypoimmune cells, researchers have combined the knockout of B2M and CIITA with the ectopic expression of HLA-E and HLA-G. Because HLA-E requires beta-2 microglobulin (B2M) for stability and cell surface expression, a fusion protein of HLA-E and B2M has been used in double-knockout (DKO) cells (Hong et al., 2025; Karaoglu et al., 2025; Li et al., 2025). This fusion protein allows proper surface presentation of HLA-E, enabling engagement with CD94/NKG2A and effectively inhibiting NK cell activity against transplanted cells. Early proof-of-concept studies demonstrated this approach in 2005, when a porcine epithelial cell line was rendered resistant to NK cell lysis by expressing an HLA-E/B2M fusion protein while knocking out endogenous B2M and CIITA (Crew et al., 2005; Heeren, 2025).

Another strategy that has been proposed to generate hypoimmune cells involves the overexpression of genes that deliver inhibitory signals to immune cells, such as CD47. CD47 is a transmembrane protein that functions as a "do not eat me" signal by interacting with

signal regulatory protein alpha (SIRPα) on macrophages, thereby inhibiting phagocytosis (Li et al., 2025; Ma et al., 2024). By engaging this pathway, cells can evade clearance by components of the innate immune system. This strategy has been combined with the suppression of HLA class I and II expression, allowing the generation and *in vivo* use of hypoimmune iPSCs differentiated into cell types such as endothelial cells and smooth muscle cells without the need for systemic immunosuppression (Koga et al., 2020). This approach aims to simultaneously reduce recognition by T lymphocytes while preventing elimination by phagocytic cells of the innate immune system. In addition to CD47, researchers have explored the expression of other inhibitory molecules that can further dampen immune responses. These include polymorphonuclear (PMN) inhibitory ligands such as CD99 and CD200, which are involved in regulating leukocyte activation and inflammatory responses (Bogomiakova et al., 2024). The combined expression of these inhibitory signals represents a promising strategy to enhance immune evasion and improve the survival of engineered cells in allogeneic transplantation settings.

2.4 Cellular delivery methods for genome editing components

During genome editing of cells, delivery methods are commonly used as vehicles to transport molecules, a process known as transfection (Chong et al., 2021a). In recent years, transfection has become increasingly popular, particularly in disease treatment and drug discovery. This technique involves the use of viral or non-viral particles to introduce exogenous material into cells; physical and chemical methods have also been employed (Chong et al., 2021a; Cohen et al., 2009). Some methods are less toxic than others, and their efficiency varies depending on the technique and cell type (Liang et al., 2015). The classification of transfection methods can be challenging due to their diversity; however, they can broadly be categorised as integrative or non-integrative, depending on whether genomic integration occurs within the host genome (Tan et al., 2019).

Integrative methods involve the insertion of external DNA into the host genome; one of the most widely used is lentivirus, which enables stable and long-term gene expression. Lentiviral vectors are widely used due to their high efficiency and ability to transduce both dividing and non-dividing cells, including primary cells (Nikcevic et al., 2003). Structurally, these viruses consist of an envelope and a capsid that protect and facilitate delivery of the viral genome into host cells (Hu et al., 2024). However, their use presents risks, including insertional mutagenesis and potential oncogenic transformation caused by the disruption of key regulatory genes. Despite these concerns, lentiviral vectors remain a powerful tool in genome engineering due to their efficiency and stability (Cerbini et al., 2015).

In contrast, non-integrative methods do not result in genomic integration and provide a safer alternative for the transient delivery of molecules into cells. Examples include adenoviruses and AAVs (Adeno-Associated Viruses), which generally exhibit lower immunogenicity compared to lentiviruses and can transduce a wide range of cell types (Fus-Kujawa et al., 2021). Chemical methods such as lipofection have also become popular; this approach uses positively charged lipid molecules to interact with the negatively charged phospholipids of the cell membrane, delivering cargo into the cytoplasm (ThermoFisher Scientific, 2018). Electroporation, a physical method, applies a brief electrical field to create temporary pores in the membrane, allowing nucleic acids or proteins to enter the cell (Chong et al., 2021a). In addition, several alternative approaches are under research, including photoporation, which uses lasers to create transient openings in the membrane, and cell-penetrating peptides (CPPs), short positively charged sequences that can form complexes with nucleic acids and facilitate cellular uptake (McGraw et al., 2024; Rádis-Baptista et al., 2017).

These delivery methods have been particularly useful in research to transfect a variety of molecules, especially DNA, RNA or small RNA or plasmid DNA (Seimetz et al., 2019). For instance, lipid nanoparticle (LNP) delivery systems have been essential for the clinical success of small interfering RNA (siRNA)-based drugs, where the RNA sequence itself is the therapeutic agent designed to silence harmful gene expression. Such drugs treat conditions ranging from hereditary amyloidosis to hypercholesterolemia and primary

hyperoxaluria. Patisiran, an intravenously administered siRNA, which is a medication approved to treat polyneuropathy caused by hereditary transthyretin-mediated (hATTR) amyloidosis, reduces abnormal protein production and is delivered in a lipid nanoparticle formulation that protects the siRNA, facilitating uptake into cells (Yu et al., 2016).

Another major application is adoptive cell therapies, such as CAR-T-cell therapy, where a patient's T-cells are genetically modified *ex vivo* (outside the body) and reinfused to target cancer cells (Li et al., 2025; Mishra & Kalyuzhny, 2024). At least two FDA-approved CAR-T therapies, Kymriah and Yescarta, use viral vectors (lentiviral or retroviral) to introduce chimeric antigen receptor genes into T cells, enabling them to recognise and destroy specific cancer cells (Seimetz et al., 2019).

The choice of delivery method in genome editing or molecular therapy depends on efficiency, specificity, toxicity, and safety considerations. Non-integrative methods are generally preferred when transient expression and minimal genomic risk are desired, while integrative methods may be used when stable long-term expression is necessary. Understanding the strengths and limitations of each delivery approach and how they have enabled real-world medicines and cell therapies is crucial for designing effective and safe therapeutic strategies.

3. Materials and Methodology

3.1 Cell Maintenance and Expansion

The healthy control human iPSC line SCTi003-A was commercially sourced from STEMCELL Technologies (SCT), having been derived by the manufacturer from peripheral blood mononuclear cells (PBMCs) of a female healthy donor, using proprietary non-integrating reprogramming methods, this cell line was chosen for carrying no known familial disease mutations, and for being fully characterised in terms of karyotype stability, pluripotency marker expression, and clearance of any reprogramming factors and vehicles.

Cells were cultured in non–cell culture-treated 6-well plates (SARSTEDT) coated with the synthetic matrix, vitronectin (10 µg/mL; STEMCELL Technologies), and maintained in mTeSR™ basal medium supplemented with mTeSR™ supplement (STEMCELL Technologies) under xeno-free, serum-free, and antibiotic-free conditions to ensure GMP compliance. During initial seeding, Thiazovivin (2 µM; STEMCELL Technologies) was added as a ROCK inhibitor to promote cell survival. Cultures were incubated in a 37 °C incubator (ThermoFisher Scientific) with a humidified atmosphere containing 5% CO_2. Incubator conditions (temperature, CO_2 and water levels) were monitored daily. To minimise contamination risk, Watershield™ (5 mL/L; Minerva Biolabs) was added to the incubator water reservoir.

Cells were passaged every five days upon reaching 70–80% confluency using 1 mL per well of ReLeSR™ (STEMCELL Technologies) and reseeded at a 1:24 split ratio onto vitronectin-coated wells. Fresh mTeSR™ medium supplemented with Thiazovivin (2 µM) was used during reseeding to enhance post-dissociation viability. The culture medium was replaced daily with 2 mL mTeSR™ per well to maintain optimal growth conditions. For specific experiments (see below), cells were seeded at the required densities in 6-, 24-, or 96-

well plates and allowed to adhere overnight before treatment. Cultures were routinely examined using an inverted microscope (NIKON TMS) to monitor morphology and confluency, and representative images were recorded and stored in designated laboratory folders. Mycoplasma contamination was assessed bi-weekly using the Mycoplasma PCR Detection Kit (abm®), and only mycoplasma-free cultures were used in subsequent experiments.

3.2 Cell Counting and Viability

To determine cell density and viability, cell counting was performed prior to each new experiment (see below). Cells were harvested by enzymatic detachment using treatment with TrypLE (Gibco) for 1.5 minutes at 37°C (optimized incubation time). The cell suspension was then centrifuged at 300 × g for 5 minutes at room temperature, and the resulting pellet was resuspended in mTeSR™ medium. An aliquot of the cell suspension was mixed with Trypan Blue dye (0.4%, Sigma Life Sciences) in a 1:1 ratio (100 of cell suspension and 100 of dye). 10 µL of this mixture was then loaded into a Neubauer counting chamber for manual cell counting.

Viable (unstained) and non-viable (blue-stained) cells were counted under a light microscope at 4× magnification, examining the four outer quadrants of the chamber. The cell concentration (cells/mL) was calculated using the following formula:

$$\frac{Cells}{mL} = \frac{Total\ number\ of\ cells\ counted}{Number\ of\ quadrants\ counted} \times dilution\ factor\ \times 10^4 \frac{cells}{mL}$$

Cell viability (%) was calculated using the equation:

$$Viability\ (\%) = \frac{Number\ of\ viable\ cells}{Total\ number\ of\ cells} \times 100$$

This procedure was repeated each time a new experimental setup was initiated to ensure consistent cell density and viability across experiments.

3.3 Cell Bank Preparation and Storage

For cryopreservation, iPSCs were cultured and passaged with TrypLE (Section 3.1). Following centrifugation and removal of the supernatant solution, iPSCs were resuspended in CryoStor® CS10 Cell Freezing Solution (Stem Cell Technologies) at a concentration of 1 × 10^6 cells/mL. The vials were gradually cooled at a controlled rate of approximately 1°C per 1 minute using a CoolCell® (Sigma-Aldrich) container placed in a –80 °C freezer for 24 hours before being transferred to long-term storage in liquid nitrogen (–196 °C).

For use in experiments, iPSC cryovials from this Working Cell Bank (WCB), created in passage six were rapidly thawed in a 37°C bead bath, cryovial decontaminated with 70% ethanol, and cells immediately transferred into pre-warmed (to room temperature) complete culture medium. The cell suspension was then centrifuged at 300 × g for 5 minutes to remove residual CryoStore solution, after which the cells were resuspended in 1 mL fresh medium supplemented with 2 µM Thiazovivin, seeded into 6-well plates coated with vitronectin (10 µg/mL) to promote attachment, and topped up with 1 mL of mTeSR plus Thiazovivin media per well. All records corresponding to each vial were maintained in the lab's cell bank inventory, and observations were documented in the laboratory database.

3.4 Cellular Transfection

3.4.1 Cellular transfection driven by cationic lipids

A 96-well plate (SARDEST) was coated with vitronectin and seeded with approximately 7,000 iPSC cells per well 24 hours prior to transfection, using the previously described cell-counting procedure. Plating was restricted to interior wells to minimise edge effects, as peripheral wells are more prone to medium evaporation and associated well-to-well variability in cell growth and assay readouts. Plating resulted in approximately 10% confluency at the time of transfection, with cells present predominantly as single cells and without colony formation. Cells were maintained overnight at 37 °C and 5% CO_2.

Twenty-four hours later, transfection was performed using Lipofectamine CRISPRMAX Cas9 Transfection Reagent (Thermo Fisher Scientific) according to the manufacturer's instructions. The experiment was designed to evaluate two variables: the amount of lipid (L) and the concentration of the ribonucleoprotein complex (RNP). The RNP complex consisted of Cas9 protein (Alt-R™ S.p. HiFi Cas9 Nuclease V3) complexed with trans-activating CRISPR RNA (tracrRNA, Alt-R™, ATTO™ 550; Integrated DNA Technologies) (see Figure 5). A crRNA was not used in this experiment as the aim was to analyse transfection efficiency via cell imaging, using only a fluorescent tracrRNA. Four different lipid conditions were tested: no lipid (L0), 0.6 µL (L1), 1.2 µL (L2), and 2.4 µL (L3), each diluted in 250 µL of Opti-MEM medium (Gibco). The lipid was then mixed with RNP complexes (composed of fluorescent tracrRNA combined with Cas9 enzyme) prepared at four different final concentrations: 0 µM (R0), 0.03 µM (R1), 0.06 µM (R2), and 0.12 µM (R3). All reaction volumes were adjusted to 250 µL using Opti-MEM and PLUS™ reagent, following the manufacturer's recommendations (Integrated DNA Technologies, 2023)

Table 1: Experimental design in a 96-well plate.

L0 and R0 represent negative control conditions with no lipid or no RNP complex, respectively. Conditions L1R1 to L3R3 correspond to a gradient of lipid and RNP concentrations. Two replicates were used per condition.

	1	2	3	4	5	6	7	8	9	10	11	12
A		R0	R0	R1	R1	R2	R2	R3	R3			
B	L0											
C	L1											
D	L2											
E	L3											
F												
G												
H												

Lipofectamine CRISPRMAX was prepared separately from the RNP complexes, as RNP assembly required a 5-minute incubation to allow complex formation between Cas9 and the ATTO-labeled tracrRNA (ThermoFisher Scientific, 2018). Subsequently, the CRISPRMAX reagent and the RNP complexes were mixed and incubated for 20 minutes at room temperature before being applied to the cells in the 96-well plate. Cells were exposed to the lipid–RNP complexes for 6 hours, after which the medium was replaced with fresh mTeSR. 24 hours later, cells were fixed with 4% paraformaldehyde (PFA) (Sigma). Nuclei were stained with 4′,6-diamidino-2-phenylindole (DAPI) (NucBlue™, Thermo Fisher Scientific). Additionally, cells were visualized using fluorescence microscopy (EVOS, Life Technologies), and images were acquired in brightfield, DAPI, RFP, and merged channels.

3.4.2 Cellular transfection driven by Cell Penetrating Peptides

Cell-penetrating peptides (CPPs) are a class of short peptides that can cross the cell membrane and deliver molecular cargo into cells (Gori et al., 2023). In this experiment, four different CPPs were tested: FAM-TAT, Arg9, CPP9, and TP10. The most relevant characteristics of these peptides are summarized in Table 1. For each CPP, six different concentrations were evaluated: 0.625, 1.25, 2.5, 5, 10, and 20 µM. These concentrations were prepared from stock solutions of 4.9 mM FAM-TAT, 2.6 mM Arg9, 0.6 mM CPP9, and 0.4 mM TP10. The experiment was performed in a 96-well plate, and the distribution of conditions is shown in Table 2. CPP solutions were prepared and added to wells containing 7,000 cells previously seeded, following the same seeding procedure described in the lipofection section. After 24 hours of incubation, cells were stained with NucBlue™ and fixed with paraformaldehyde. Finally, cells were visualized using fluorescence microscopy, as described above.

Table 2. Cell-penetrating peptides chemical features

NAME	AA SEQUENCE	WEIGHT	STOCK (MM)
FAM-TAT	FAM-ahx-YGRKKRRQRRR-OH	2031.29	4.9
FAM-ARG9	FAM-ahx-RRRRRRRRRR-OH	1895.15	2.6
FAM-CPP9	H-cyclo(K((FAM)f-[2Nal]-RrRrQ)-OH	1583.75	0.6
FAM-TP10	FAM-ahx-AGYLLGKINKLALAALAKKIL-NH2	2653.21	0.4

Table 3. Experiment planning for CPP assessment. Four different CPPs were tasted at a gradient concentration from 0.625 to 20 µM. Note that the negative control used the CPP diluent only, to evaluate cell toxicity.

96-WELL PLATE VIEW

	1	2	3	4	5
	NEGATIVE				
A	CONTROL	TAT (µM)	Arg9 (µM)	CPP10 (µM)	TP10 (µM)
B	NA	20	20	20	20
C	NA	10	10	10	10
D	NA	5	5	5	5
E	NA	2.5	2.5	2.5	2.5
F	NA	1.25	1.25	1.25	1.25
G	NA	0.625	0.625	0.625	0.625
H					

3.4.3 Cellular transfection driven by photoporation

First, the cells were counted using an automated cell counter to determine the appropriate seeding density. A 96-well plate was seeded with 25,000 cells per well in complete growth medium. The plate was incubated overnight at 37 °C in a humidified incubator with 5% CO_2 to allow the cells to attach and reach the desired confluency. The following day, the LumiPore device (Trince) was set up by selecting the appropriate cell type, nanosensitizer (LS2-C), laser parameters, and the 96-well plate format in the software interface. The laser intensity was adjusted to 80% or 40% of the maximum output, according to the experiment optimization settings selected.

In parallel, the LS2-C nanosensitizer was prepared by diluting the stock solution 1:100 in ultrapure water. From this intermediate dilution, additional working dilutions were prepared at 50×, 25×, 12.5×, and 6.25×. Prior to the photoporation experiment, the cell culture medium was replaced with Opti-MEM to enhance delivery efficiency and reduce serum interference. The LS2-C working dilutions were prepared using Opti-MEM as the diluent. The cargo molecule, FITC-Dextran, was diluted to a final concentration of 5 µM in Opti-MEM. The nanosensitizer and cargo solutions were then added to the cells immediately before laser treatment according to the optimized photoporation protocol.

3.5 HPRT, B2M and CIITA knockout

As described in section 3.4.1, CRISPRMAX was used as the transfection reagent, and Cas9 was complexed with single-guide RNA (sgRNA) before transfection. To generate the sgRNA, trans-activating CRISPR RNA (tracrRNA) and the corresponding CRISPR RNA (crRNA) for B2M, CIITA, and HPRT (Integrated DNA Technologies; see Table 4 for crRNA sequences) were mixed at a 1:1 molar ratio and annealed by incubation at 95 °C for 5 minutes. Transfections were performed in Opti-MEM medium using Lipofectamine CRISPRMAX, applying the L1R3 conditions (Figure 8, D) previously described and adapted to a 24-well plate format, corresponding to 7.2 µL of Lipofectamine and an RNP final concentration of 0.12 µM. After 6 hours of transfection, the medium was replaced with mTeSR. Twenty-four hours later, cells were dissociated using TrypLE, and genomic DNA was extracted using the GeneJET Kit as described below. DNA samples were subsequently submitted for Sanger sequencing using the forward and reverse primers designed as described below.

3.6 crRNA off-target binding analysis

Potential off-target sites for each crRNA were identified using the CRISPR RGEN Cas-OFFinder tool (http://www.rgenome.net/cas-offinder/). This bioinformatic tool compiles 23-bp sequences composed of the 20-bp sgRNA and the 3-bp PAM region against the genome of interest. First, the tool identifies the query sequence and the PAM region in the genome and compares these sites to find mismatched bases. Then, Cas-OFFinder selects sequences with fewer mismatches according to a threshold and reports the genomic locations of these sequences, allowing assessment of CRISPR specificity and minimization of unintended genomic modifications.(Bae et al., 2014).

3.7 Genomic DNA extraction

Two kits were evaluated for genomic DNA extraction from iPSC; GeneJET Kit (Thermo Scientific) and DNA Extract All Reagents (Thermo Fisher). Cells seeded in multi-well plates were harvested and transferred to Eppendorf tubes, and DNA was extracted using the two kits, based on manufacturer's instructions. Briefly, the GeneJet Kit included sample lysis, followed by treatment steps in which proteins and RNA were degraded using proteinase K (56^{o}C for 10 minutes) and RNase (room temperature for 10 minutes), respectively. Then, alcohol was added to precipitate DNA, and multiple centrifugation cycles performed to bind gDNA to a silica column and purify the molecule, before eluting purified gDNA into a microcentrifuge tube. In contrast, the DNA Extract All Reagents kit required only a lysis and a stabilization solution to obtain a PCR-ready product, without requiring use of silica columns for product purification.

3.8 DNA quantification

Following transfection experiments, DNA extraction was evaluated using a NanoDrop 1000 microvolume UV-Vis spectrophotometer (ThermoFisher Scientific) to determine DNA concentration and purity. Only those samples with DNA with 260/280 ratio between 1.7 – 1.9 was accepted for use in subsequent experiments.

3.9 PCR primer design

Bioinformatic tools were primarily used to design primers. Primers were designed to target B2M, CIITA, and HPRT to verify the success of gene knockout. Each primer was specifically designed to amplify the region targeted by the corresponding CRISPR RNA (crRNA), enabling confirmation of successful gene disruption. The first step involved identifying the

genomic locations of each crRNA using information provided by the manufacturer (Integrated DNA Technologies). The genomic coordinates for the three crRNAs targeting B2M, CIITA, and HPRT were visualized using the NCBI Genome Data Viewer in the human genome GRCh38 (http://ncbi.nlm.nih.gov/gdv). After locating the targeted genomic regions, the crRNA sequences were aligned to the corresponding genomic sequences using Clustal W version 2.1 (https://www.genome.jp/tools-bin/clustalw), a general-purpose multiple alignment program for DNA and proteins, to confirm that each crRNA matched the intended locus.

Primers were then designed using online tools, including IDT PrimerQuest (https://eu.idtdna.com/pages/tools/primerquest) and VectorBuilder Primer Design (https://en.vectorbuilder.com/tool/primer-design.html). Primer selection was based on sequence specificity, melting temperature, GC content, and expected product size. All primer sequences (Table 4) were aligned to the previously identified target regions to ensure proper binding.

Table 4. crRNA and PCR primer sequences, and primer properties

Gene	Orientation	crRNA sequence	Sequence	Tm (°C)	GC content (%)	Molecular Weight (Da)	DNA bases	Product size (bp)
HPRT	Forward	5'-AATTATGGGGATTACTAGGA-3'	5'-ACAGAGCGAGATTCCGTCT-3'	55.6	52.6	5812.8	19	428
HPRT	Reverse		5'-CAGAGAGACTACAGGGCATT-3'	53.7	50	6175.1	20	
B2M	Forward	5'-AAGTCAACTTCAATGTCGGAGTTTTAGAGCTAGAAA TAGCAAGTTAAAATAAGGCTAGTCCGTTATCAACTTGA	5'-TGGTGCCTGATATAGCTTGA-3'	53.3	45	6163	20	468
B2M	Reverse	AAAAGTGGCACCGAGTCGGTGCTTTT-3'	5'-ATTCAGGGTAGTATGCCAT-3'	53.1	45	6172.1	20	
CIITA	Forward	5'-CCGTGGACAGTGAATCCACTGTTTTAGAGCTAGAAATA GCAAGTTAAAATAAGGCTAGTCCGTTATCAACTTGAAAAA	5'-TCCAGGAGCTAGATGTAACTC-3'	53.1	47.6	6430.2	21	529
CIITA	Reverse	GTGGCACCGAGTCGGTGCTTTT-3'	5'-GATGGCTGTATTTGGATGGG-3'	53.5	50	6259.1	20	

3.10 Polymerase chain reaction (PCR)

PCR reaction conditions were optimized using OneTaq Quick-Load 2X MM with Standard Buffer (NEB) and a primer mix targeting the genes indicated in Table 4. PCR reaction mix conditions are summarized in Table 5. Gradient PCR, in the presence or absence of GC enhancer solution (NEB) was initially performed, to identify optimal amplification conditions for each primer set, via testing six annealing temperatures ranging from 49.1 to

56.9 ºC. DNA was loaded onto 1% agarose gels (SIGMA) prepared in TAE buffer, with a 1000 bp GeneRuler DNA ladder (Thermo Fisher) and Midori Green DNA binding agent (NIPPON). Electrophoresis was performed at 125 V for 40 minutes, in TAE buffer. Agarose gels were imaged using GelDoc™ EZ Imager (BIO-RAD).

Table 5.PCR reaction mix conditions using One Taq Quick-Load mix

Component	25µl reaction	Final Concentration
10 µM Primer Mix	1 µl	0.2 µM
200 ng/ul Template DNA	5 µl	<1000ng
One*Taq* Quick-Load 2X MM with Standard Buffer	12.5 µl	1X
Nuclease-free water	6.5 µl	
Total	25	

Table 6. Thermocycler conditions for the gradient PCR

STEP	**TEMP**	**TIME**
Initial Denaturation	94°C	30 seconds
30 Cycles	94°C	20 seconds
	49.1-56.9°C	30 seconds
	68°C	30 sec
Final Extension	68°C	5 minutes
Hold	4-10°C	

3.11 PCR product purification and Sanger sequencing

PCR products were purified using the NucleoSpin Gel and PCR Clean-up kit (Macherey-Nagel). Briefly, the PCR sample was adjusted to 50 µL with nuclease-free water and mixed

with NTI buffer. The mixture was loaded onto a NucleoSpin column and centrifuged at 11,000 × g for 30 s, and the flow-through was discarded. The column was washed twice with NT3 buffer and centrifuged after each wash. A final centrifugation step was performed to remove residual buffer. DNA was eluted with 15 µL of NE buffer after a 1 min incubation at room temperature, followed by centrifugation. DNA concentration was measured, and samples were diluted to 5 ng/µL for sending to Eurofins, using the Mix2Seq kitbox. Sanger sequences results were visualized using Chromas version 2.6.6

3.12 Image processing

All images acquired through fluorescence or phase-contrast/brightfield microscopy were analysed to assess cell confluency and transfection efficiency. ImageJ (64-bit, version 1.8.0) was used to systematically and uniformly adjust image parameters, including labels, brightness, contrast, shadows, and obtain object measurements in pixels ImageJ allowed the application of two previously set thresholds; Phansalkar and Huang 2. These image adjustments replace pixels, separating the background from the object. This allows pixels to be classified depending on image intensity and a threshold, making images uniform for further adjustments (Tizhoosh, 2005). Additional software, such as CellProfiler (version 4.2.8), was employed to quantify cytoplasmic and nuclear areas and to create customizable workflows for image processing, such as background subtraction, segmentation, and feature extraction. Furthermore, the Catapult Cell Confluency Tool, an image processing tool available at https://ct.catapult.org.uk/resources/confluency-tool, was used as an orthogonal method for estimating cell confluency. Confluency was quantified as a percentage of the captured culture surface area occupied with cells. Examples of processed images and workflows generated with these tools are shown in Figure 5.

Image quantification was carried out using a combination of Image g, Catapult and Cell Profiler. Cell confluency was estimated by calculating the area of contrast between the

background (lighter pixels) and the cells (represented by darker pixels) and multiplying this number by 100 to represent values as a percentage.

$$Confluency\ \% = \frac{Number\ of\ Cell\ pixel}{Total\ image\ pixels} \times 100$$

Additionally, transfection efficiency, known as the number of cells successfully transfected compared with the total number of cells, was calculated by counting the total number of cells the DAPI (Blue signs) overlapped with the fluorescent CPP (Green signal) and divided by the total number of cells in the image. A similar approach was used for the Lipofectamine experiment (see Figure 8), but using the fluorescent marker of the RNP (Red signal).

$$Transfection\ efficiency\ \% = \frac{Number\ of\ cells\ transfected}{Total\ number\ of\ cells} \times 100$$

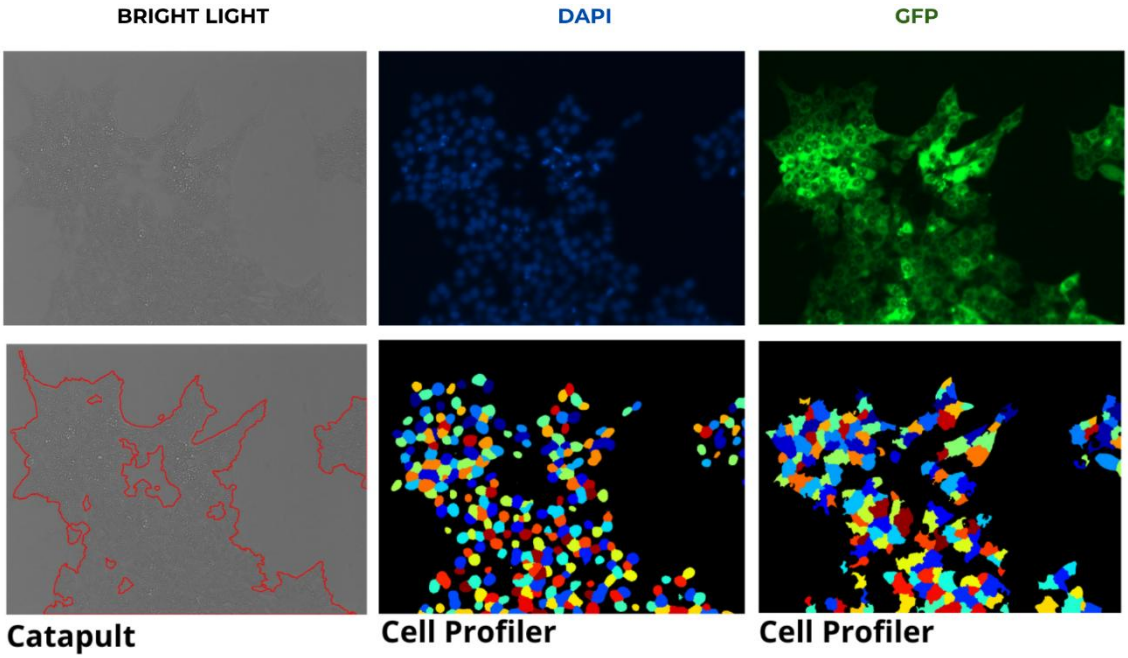

Figure 5. Cell images processing

Representative bright-field and fluorescence images processed using Cell Profiler to quantify nuclei numbers and cytoplasm areas, and Catapult Cell Confluency Tool for cell confluency assessment.

3.13 Statistical analysis

All statistical analyses of processed images were performed using SPSS version 09.0.2.0 and GraphPad Prism 10.5.0. Descriptive statistics, including mean and standard deviation (SD), were calculated for each dataset. Comparisons between two groups were performed using unpaired or paired t-tests, depending on the experimental design, while comparisons among three or more groups were conducted using one-way or two-way ANOVA analysing the transfection efficiency results per CPPs (Section 4.9) followed by appropriate post hoc tests (e.g., Tukey's or Bonferroni) to identify significant differences between groups. Results are presented as mean ± SD, and a p-value < 0.05 was considered statistically significant. All analyses assumed normal data distribution, and assumptions were checked prior to statistical testing.

3.14 Illustrations

All Illustrations were created using BioRender (https://www.biorender.com/).

4. Results

4.1 iPSC culture and banking

iPSC were cultured in mTeSR™ Complete, a serum-free and feeder-free medium specifically formulated for human pluripotent stem cells. The cell line SCTi003-A exhibited rapid proliferation, and between 500,000 and 700,000 cells were seeded per well in a six-well plate to achieve 70-80% confluence by day 5. Throughout multiple passages and reseeding procedures, the cells maintained morphological characteristics consistent with an undifferentiated phenotype, growing as compact, tightly packed cobblestone-like colonies with smooth, well-defined borders, little intercellular space, and small round/oval cells with high nucleus-to-cytoplasm ratio. As expected (Castro-Viñuelas et al., 2021), an increasingly homogeneous undifferentiated morphology was observed with successive passages (Figure 6) post-thaw. Following culture on vitronectin-coated plates with TrypLE™ dissociation for two passages, iPSC were cryopreserved to create a WCB comprised of a total of 10 cryovials.

4.2 Optimisation of enzymatic passaging time

Prior to iPSC expansion and banking, enzymatic passaging time with TrypLE and coating matrix were optimized to ensure optimal growth conditions would be used to create a WCB for use in subsequent experiments.

For TrypLE, treatment durations of 1, 1.5, and 2 minutes were tested. Excessive exposure to TrypLE™ (≥2 minutes) resulted in reduced cell viability and morphological alterations. Conversely, TrypLE™ exposure for < 1.5 minutes was not sufficient to allow dissociation of iPSC colonies into single cells without excessive pipetting. Therefore, an optimal dissociation time of 1.5 minutes was established to preserve cell integrity and proliferation capacity. Figure 6 shows representative images from the cell culture optimization process.

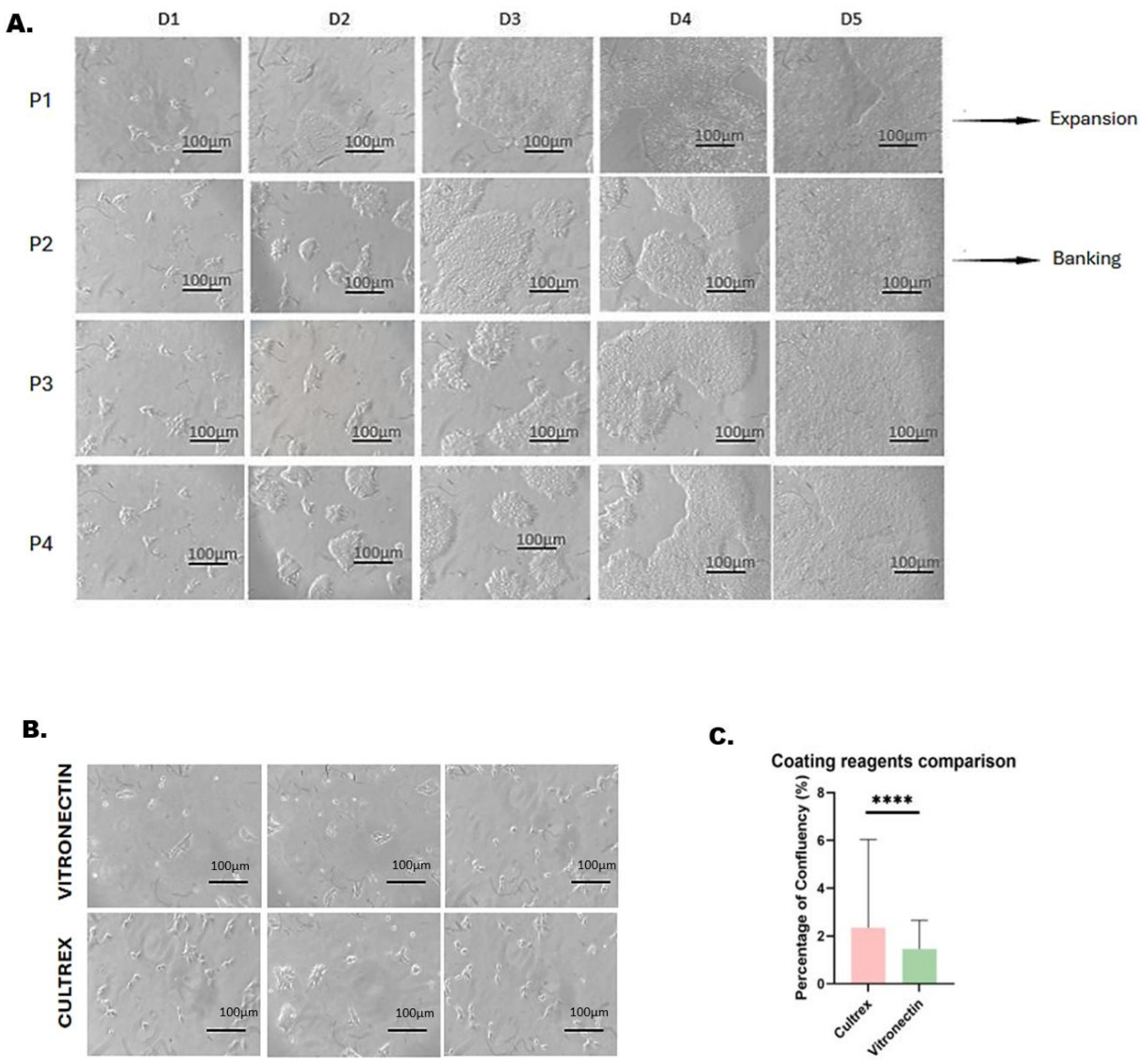

Figure 6. SCTi003-A Cell Line Culture Optimization.

A) Phase-contrast images of cell culture, showing daily (D1 to D5) iPSC morphology and confluence over six passages. B) Comparison between the coating reagents Vitronectin and Cultrex. C) Cell culture images from two different conditions: one with Vitronectin and the other with Cultrex.

4.3 Optimisation of coating reagent

Cultrex, an animal-derived non-defined matrix purified from the Englebreth-Holm-Swarm murine tumor and used as gold standard for iPSC culture , and Vitronectin XF, a recombinant serum and extracellular matrix glycoprotein (R&D Systems, n.d.; STEMCELL Technologies, n.d.), were evaluated to determine whether they influenced cell confluency. Statistical analysis revealed significant differences between Cultrex and Vitronectin XF, with higher confluency observed in Cultrex-coated wells (2.3% ± 3.7%) compared to vitronectin-coated wells (1.453% ± 1.2%). This comparison was performed in a 24-well plate format, with 300,000 cells seeded per well and confluency measured 24 hours after seeding. Moving forward, it was decided that Vitronectin FX could support routine iPSC culturesbecause it is compatible with GMP practices, i.e., has available chemical composition and is Animal-Origin Free (AOF) and Xeno-Free. In contrast, the superior Cultrex matrix was used during genetic modification experiments when iPSCs required additional support for clonal expansion.

4.4 Optimisation of DNA extraction from iPSC

To prepare for genetic modification experiments, DNA extraction from iPSCs was optimised using cells pelleted from routine cultures to determine whether a buffer-based system (DNA Extract All Reagents; Thermo Fisher Scientific) could replace standard column-based DNA extraction (GenJet; Thermo Fisher Scientific) as a cost- and time-effective alternative. DNA Extract All Reagents kit, was tested with cell samples at room temperature or warmed to 95 °C to facilitate extraction. Following extraction, DNA concentration and purity were quantified using a NanoDrop spectrophotometer.

Samples extracted with the DNA Extract All Reagents kit showed incomplete purification (multiple absorption peaks). The 260/280 ratio was 0.89 for samples that were warmed and

0.83 for samples extracted at room temperature (Figure 7A). In contrast, DNA extracted using the GenJet kit showed greater purity (single absorption peak), with a 260/280 ratio of 1.77.

To further evaluate the quality of extracted DNA, PCR amplification of the control gene HPRT (1083 bp) was performed using a commercially validated primer mix procured through IDT. PCR products from three conditions; DNA Extract All Reagents at 95 °C, DNA Extract All Reagents at room temperature, and GenJet were analyzed on an agarose gel. Two positive control DNA samples were included in the PCR reaction. The results demonstrated that only the GenJet-purified DNA yielded successful amplification (Figure 7B), while both DNA Extract All Reagents samples did not show visible DNA bands. Based on these findings, the GenJet kit was used for DNA extraction in subsequent experiments, despite its higher time and cost requirements.

A.

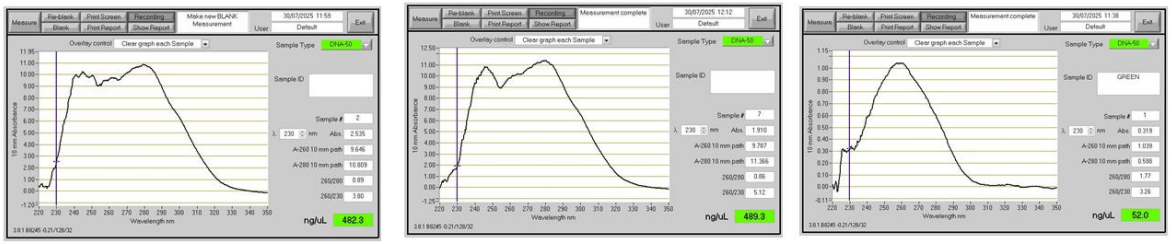

SCTi003-A iPSC P6 gDNA

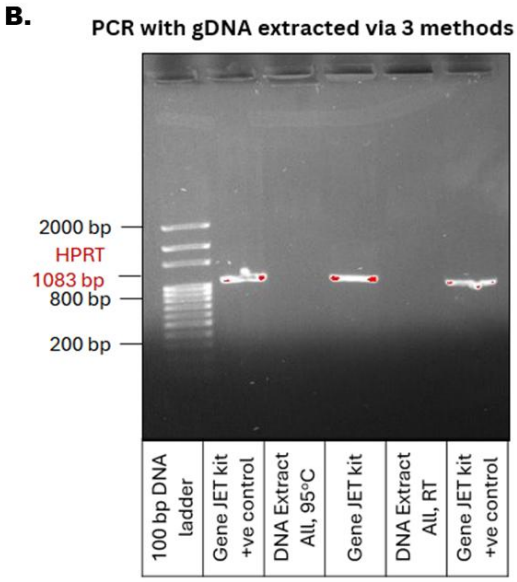

Figure 7. DNA extraction using three different methods.

A) Spectrophotometric profiles of DNA extracted using three different methods: DNA Extract All Reagents kit with sample heating at 95 °C, DNA Extract All Reagents kit with samples at room temperature, and GeneJET DNA Extraction Kit . B) Agarose gel electrophoresis showing DNA amplification from GeneJET Kit extraction. The DNA ladder is displayed on the right, flanked by two positive controls (DNA samples previously tested for HPRT amplification), with the HPRT sample of interest in the centre.4.5 Optimisation of CRISPR/Cas9 component delivery to iPSC via lipofection

Following cell culture, DNA extraction, and PCR optimisation, a transfection experiment was performed to determine the optimal concentrations of CRISPRMAX and the ribonucleoprotein (RNP) complex for high transfection efficiency while maintaining cell survival. Sixteen conditions were evaluated, with L0 and R0 representing no lipid and no RNP. Lipid concentrations (L1–L3) increased by 1.2%, 2.4%, and 4.8%, respectively, while RNP concentrations (R1–R3) were 3%, 6%, and 12% of the total reaction volume (see Figure 8D for details of volumes used).

As shown in Figure 8, increasing CRISPRMAX and RNP concentrations resulted in reduced cell survival and fewer colonies, which correlated with decreased confluency. Conversely, transfection efficiency generally increased with higher lipid and RNP concentrations, although this occurred alongside increased cytotoxicity. Lipid concentrations above 1.2% were more toxic, as indicated by a relative decrease in cell confluency compared to the L0R0 control. For example, L2 conditions reduced confluency by 47–69.9%, while the most cytotoxic combination, L3R2, decreased confluency by approximately 80%. These results suggested that L1 (1.2% lipid) was the most suitable condition for transfection, as cell proliferation remained largely unaffected.

Transfection efficiency was assessed across all sixteen treatments using image-based analysis under two threshold methods (Phansalkar and Huang 2; see section 3.12). Both methods showed an overall increase in efficiency with higher lipid/RNP concentrations, with some exceptions (L2R2 in Figure 8A and L3R1 in Figure 8B). Conditions L0R0 to L0R3 showed a small percentage of transfected cells despite the absence of lipid, likely due to RNP being positioned near the cell membrane without successful uptake. The L1R3 condition yielded the highest transfection efficiency, reaching approximately 40% and over 50% with the Phansalkar and Huang 2 thresholds, respectively.

Representative images in Figure 8 illustrate cell toxicity and transfection outcomes at the highest lipid and lowest RNP concentrations. Overall, L1R3, corresponding to 1.2% lipid and 12% increase of the RNP concentration, appeared to be the most suitable condition for future transfections, as it provided low cytotoxicity with high transfection efficiency.

A.

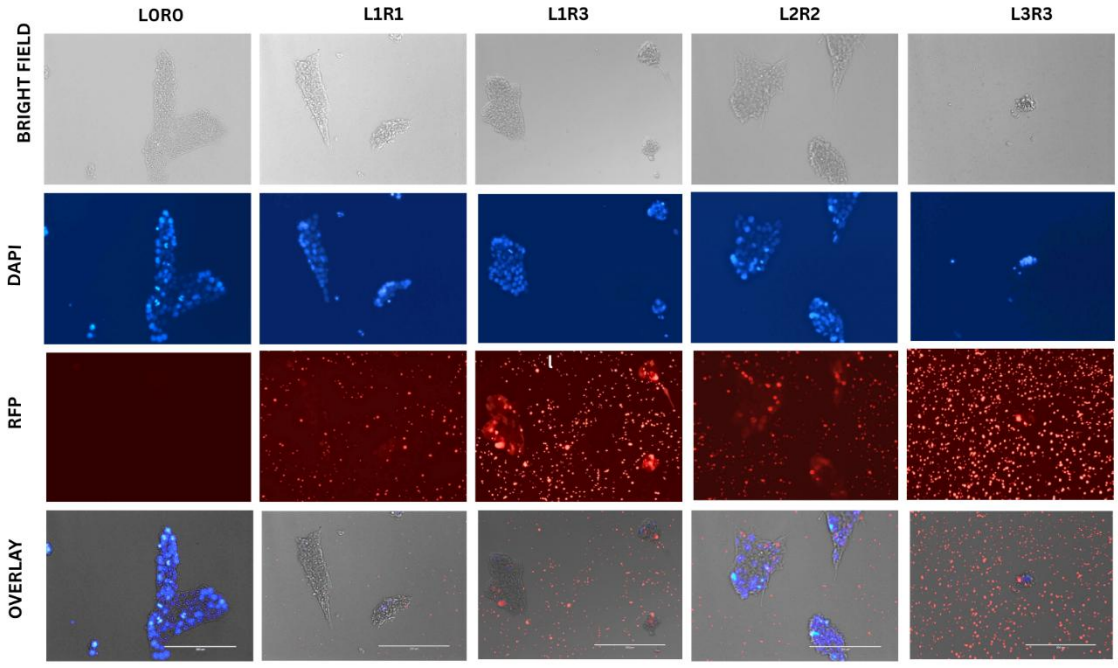
L0R0
L1R1
L1R3
L2R2
L3R3
BRIGHT FIELD
DAPI
RFP
OVERLAY

B.

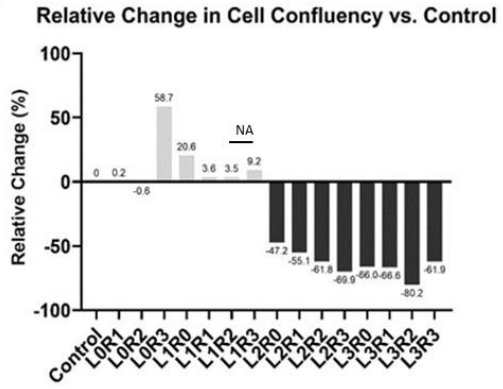
Relative Change in Cell Confluency vs. Control
Relative Change (%)
100
50
0
-50
-100
0
0.2
-0.6
58.7
20.6
3.6
3.5
NA
9.2
-47.2
-55.1
-61.8
-69.9
-66.0
-66.6
-80.2
-61.9
Control
L0R1
L0R2
L0R3
L1R0
L1R1
L1R2
L1R3
L2R0
L2R1
L2R2
L2R3
L3R0
L3R1
L3R2
L3R3

C.

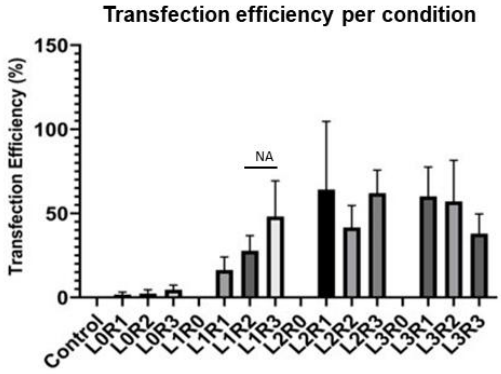
Transfection efficiency per condition
Transfection Efficiency (%)
150
100
50
0
NA
Control
L0R1
L0R2
L0R3
L1R0
L1R1
L1R2
L1R3
L2R0
L2R1
L2R2
L2R3
L3R0
L3R1
L3R2
L3R3

D.

Treatment	RNP (µl)	C-MAX (µl)
L0R0	0	0
L0R1	0.75	0
L0R2	1.5	0
L0R3	3	0
L1R0	0	0.6
L1R1	0.75	0.6
L1R2	1.5	0.6
L1R3	3	0.6
L2R0	0	1.2
L2R1	0.75	1.2
L2R2	1.5	1.2
L2R3	3	1.2
L3R0	0	2.4
L3R1	0.75	2.4
L3R2	1.5	2.4
L3R3	3	2.4

RNP: Ribonucleoprotein complex volume (crRNA and Cas9 1:1) C-MAX: Lipofectamine CRISPRMAX

Figure 8. Transfection condition optimisation.

A) Cell images showing brightfield, DAPI, RFP, and merged channels for the negative control and four representative conditions from the fifteen evaluated in the experiment. An illustration depicts the components of the cargo: a CRISPRMAX lipid nanoparticle containing the Cas9 enzyme and a fluorescently labelled tracrRNA. B) Relative changes in transfection and cell survival compared to the negative control for all fifteen treatments. C) Transfection efficiency percentage per treatment n = 16. D) Outline of the Lipid, Cas9 and gDNA conditions used per treatment (n = 18), each in a total of 50 µl of total reaction volume.

Using the previously optimised L1R3 condition, a follow-up experiment was performed to transfect iPSCs with CRISPRMAX and the RNP complex, in order to confirm that this condition maintained high transfection efficiency without excessive cytotoxicity. Analysis of images revealed a transfection efficiency of 24.25% ±20%, lower than the initial optimization experiment 48.07% (Figure 9 B-C). Cell confluency was also reduced, with a mean of 11%

±15%. High standard deviation was due to uneven cell distribution, with areas of high cell density interspersed with regions containing few or no cells. Despite this variability, the observed transfection efficiency (calculated as the number of cells showing blue fluorescence over the red fluorescent RNA signals, vs. the total cells showing blue fluorescence signal) was still comparable to that of the L1R2 condition, previously reported at 27.71%. Notably, no statistically significant difference was observed between L1R2 and L1R3 (Figure 9), indicating that both conditions achieved similar transfection outcomes.

A.

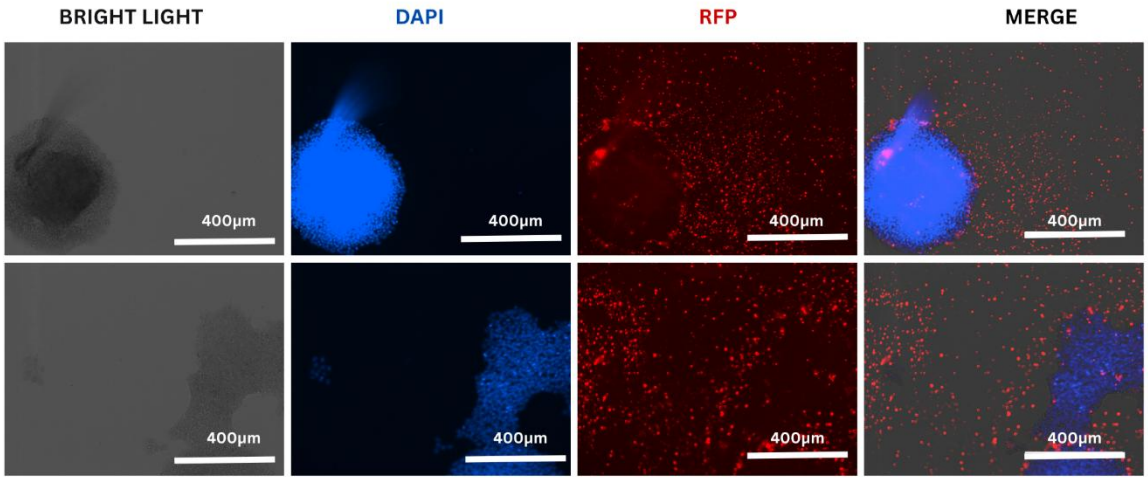
BRIGHT LIGHT
DAPI
RFP
MERGE
400µm

B.

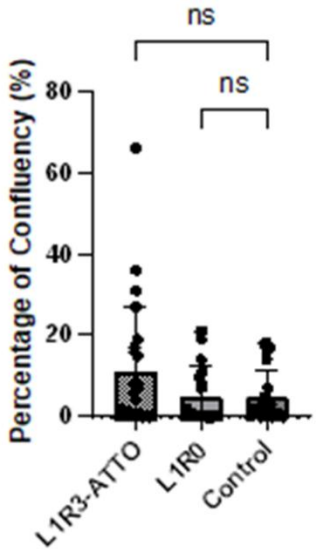
ns
ns
Percentage of Confluency (%)
0
20
40
60
80
L1R3-ATTO
L1R0
Control

C.

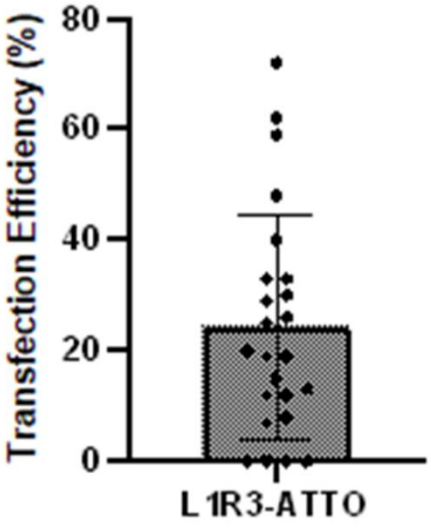
Transfection Efficiency (%)
0
20
40
60
80
L1R3-ATTO

Figure *9*. Transfection using the L1R3 condition.

A) The images show the results of the transfection experiment after L1R3 was identified as the optimal condition for transfection efficiency and cell survival. B) Bar graph showing a confluency of approximately 15% and C) transfection efficiency of about 23% under condition L1R3 (n=18). Black dots in B and C represent replicate measurements of confluency and transfection efficiency, respectively.

4.6 Optimisation of PCR amplification with HPRT, B2M, and CIITA custom primers

Prior to lipofection for knock-out experiments targeting *HPRT* (intended as positive control), *B2M*, and *CIITA*, PCR primers surrounding the genomic loci identified by crRNAs were used. PCR mixes were prepared for each primer set with and without using a GC enhancer reagent and gradient PCR was performed to determine the most appropriate annealing temperature. The gradient PCR was set from 49.1 to 56.9 °C for *HPRT*, *B2M*, and *CIITA*.

Results showed that only *HPRT* amplification improved with the addition of the GC enhancer reagent (Figure 10B). No significant difference was observed for *B2M*. In the *CIITA* sample, the banding pattern appeared altered compared to the non-GC enhancer treatment, possibly due to the effect of the GC enhancer on amplification specificity (Guido et al., 2016). Under these buffer conditions, single PCR bands of the expected size were generated for each gene. Optimal amplification temperatures were 51.4°C for *HPRT*, *B2M*, and *CIITA*. This experiment confirmed best DNA amplification conditions for each gene, which could subsequently be used for gDNA amplification and Sanger sequencing to assess gene knockout.

4.7 Lipofection of B2M and CIITA gRNAs into iPSC for gene knock-out

According to these results, L1R3 or L1R2 can be used to transfect iPSCs without significant effects on cell survival while maintaining considerably high transfection efficiency. Based on these findings, the knockout of *HPRT* (intended as a positive control), *B2M*, and *CIITA* was performed using these conditions, adapted to a 24-well plate format with three replicates per condition. This setup ensured sufficient DNA yield for extraction and sequencing under the previously optimised conditions.

Twenty-four hours after lipofection, cells were fixed and assessed for confluency. A confluency percentage of ~15% was reported for *CIITA*, *B2M*, and *HPRT*. No statistically significant differences were found among the three samples, with standard deviations of 7.1%, 5.6%, and 5.4%, respectively. Figure 10A shows representative images of this experiment. Subsequently, DNA was extracted using the GeneJET kit, and PCR was performed for all three samples using the previously designed primers for *B2M*, *CIITA*, and *HPRT*. The results showed a single band for each gene: 428 bp for *HPRT*, 393 bp for *B2M*, and 529 bp for *CIITA*, demonstrate that DNA was successfully extracted and that the primers specifically amplified the intended target regions (Figure 10C).

A.

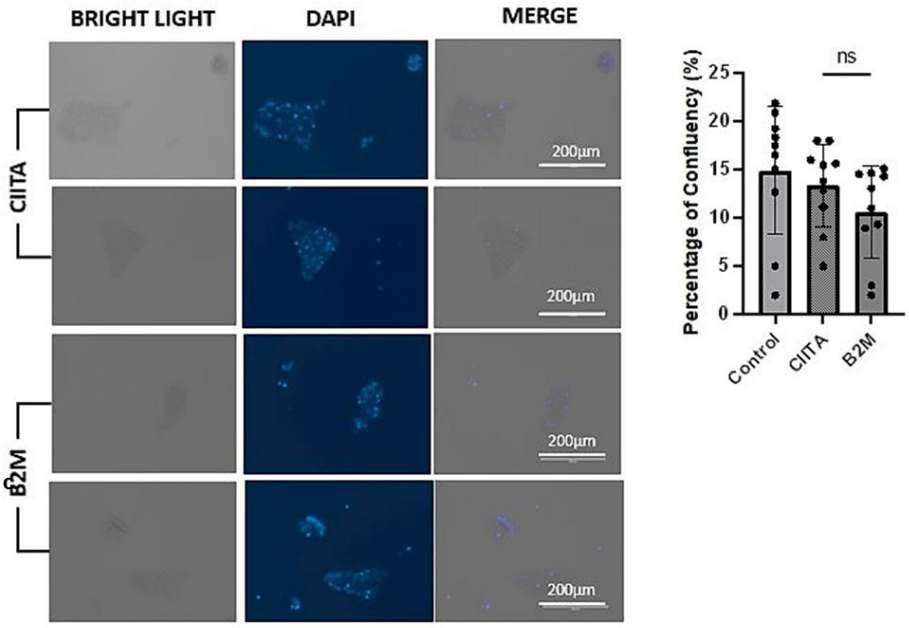
BRIGHT LIGHT
DAPI
MERGE
CIITA
B2M
200µm
200µm
200µm
200µm
Percentage of Confluency (%)
25
20
15
10
5
0
ns
Control
CIITA
B2M

B.

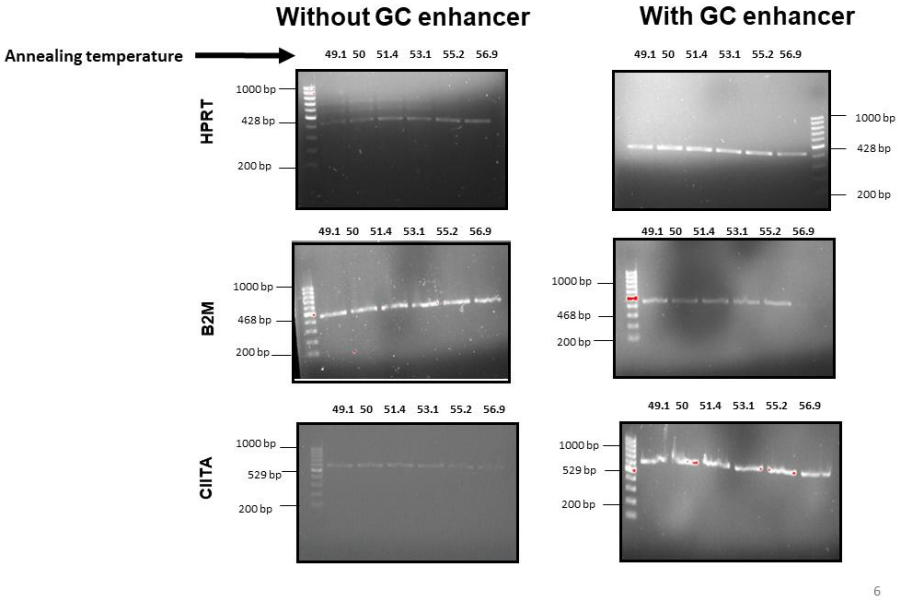
Without GC enhancer
With GC enhancer
Annealing temperature
49.1 50 51.4 53.1 55.2 56.9
HPRT
1000 bp
428 bp
200 bp
B2M
1000 bp
468 bp
200 bp
CIITA
1000 bp
529 bp
200 bp

6

C.

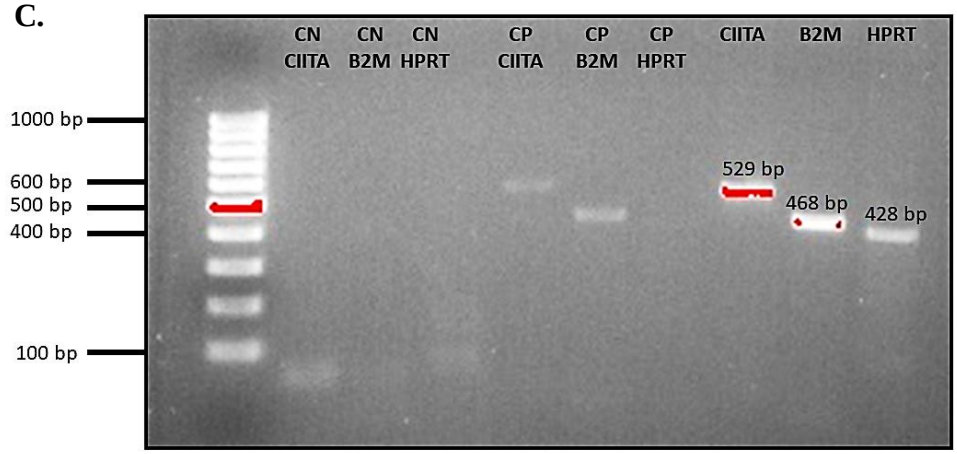
CN CIITA
CN B2M
CN HPRT
CP CIITA
CP B2M
CP HPRT
CIITA
B2M
HPRT
1000 bp
600 bp
500 bp
400 bp
100 bp
529 bp
468 bp
428 bp

D.

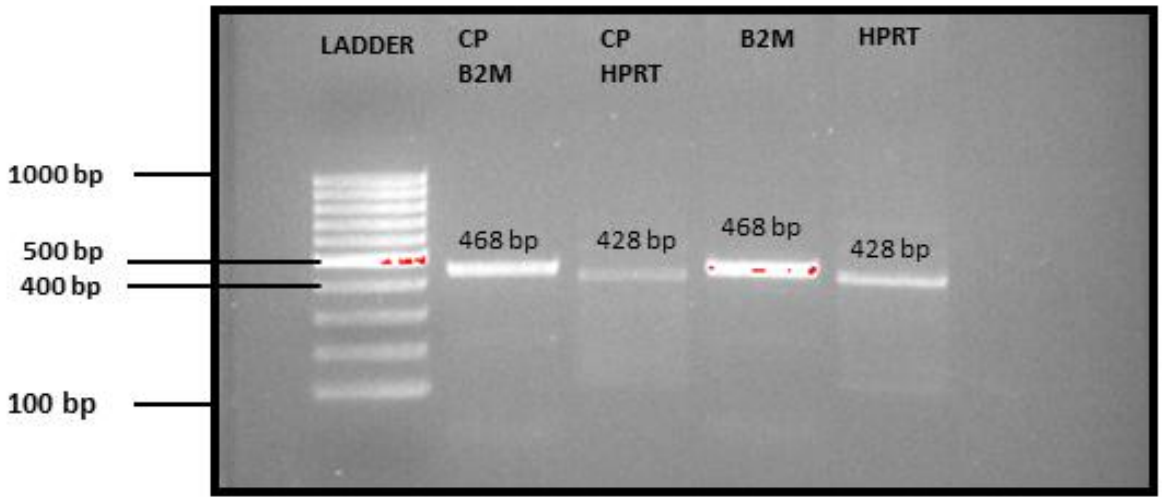
LADDER
CP B2M
CP HPRT
B2M
HPRT
1000 bp
500 bp
400 bp
100 bp
468 bp
428 bp
468 bp
428 bp

Figure 10. HPRT, B2M and CIITA knock-outs.

A) Representative pictures showing a cell survival assay after RNP-CRISPRMAX exposure in iPSCs, a negative control was included, and the percentage of confluency measured was respectively 13.8% (CIITA) and 11% (B2M), respectively. The t-test showed no statistically significant difference between treatments. B) Gel electrophoresis was performed for HPRT, B2M and CIITA; a GC enhancer was used to avoid non-specific amplifications. C) Gel electrophoresis to test primers designed for CIITA, B2M, and HPRT. CP: Positive Control (DNA sample); CN: Negative Control. D) An additional electrophoresis was performed to test CP HPRT, which was not amplified in C).

A total of eight samples were submitted for Sanger sequencing, corresponding to the three genes evaluated in both forward and reverse directions, as well as a non-edited control sample evaluated in both forward and reverse directions. PCR products were purified using the NucleoSpin Gel and PCR Clean-up kit (Macherey-Nagel). Post-purification, four spectrophotometer measurements were performed per sample, and values were averaged to obtain more accurate data. 260/280 ratios were 1.83 for *HPRT* and *B2M*, and 1.89 for *CIITA*. All 260:280 ratios were higher post-purification, and absorbance peaks were smoother, reflecting successful purification. Sanger sequencing results, followed by ICE tool analysis that can detect even small percentages of genome edited within mixed cell populations (EditCo's, 2026) did not show evidence of a knockout at the target loci of any of the genes. These results indicate that, under the tested conditions, the desired gene disruptions were not detected (Figure 11).

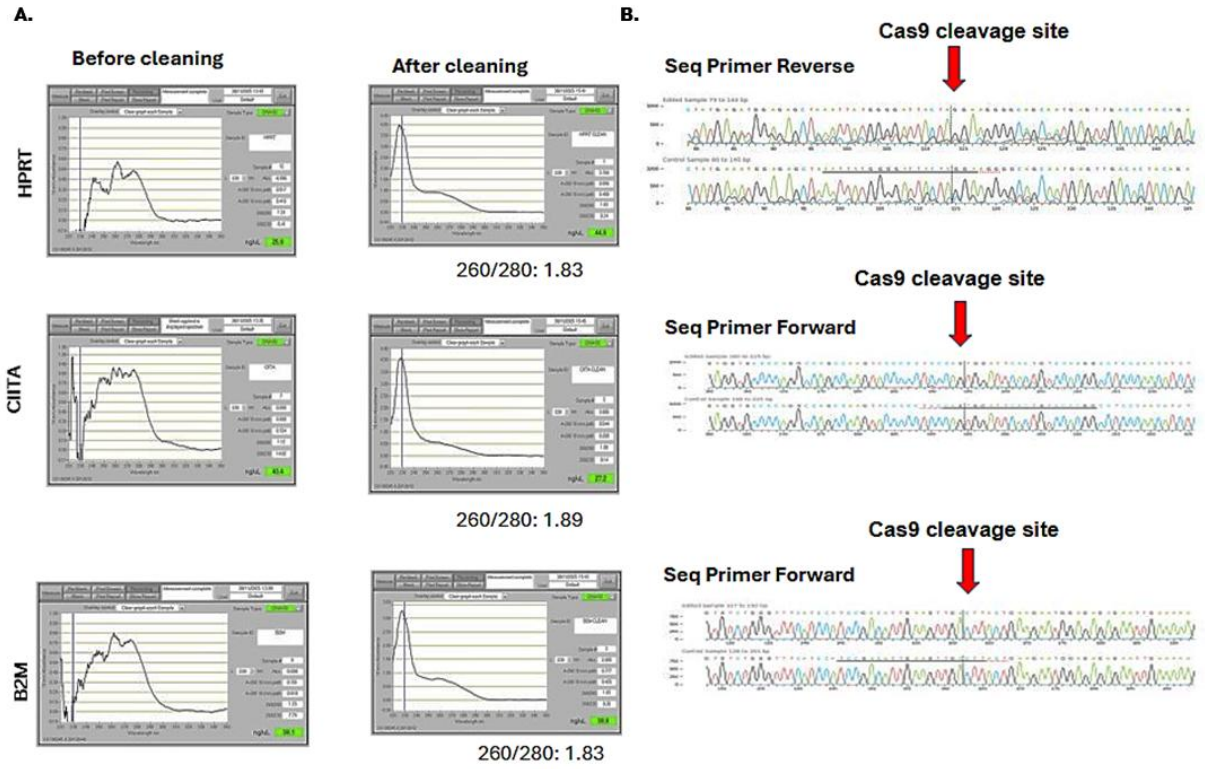

Figure 11. PCR-Cleaning and Sanger sequencing results.

A) DNA concentrations for HPRT, CIITA, and B2M were measured using a spectrophotometer. B) Knockout results, shown from top to bottom: Reverse primer for HPRT, forward primer for CIITA, and B2M; two lines of traces shown to represent full sequencing result per sample.

4.8 Cargo delivery to iPSC *via* photoporation

In order to further optimize cargo delivery to iPSC and achieve a knockout, additional transfection techniques in iPSCs were employed, including delivery mediated by photoporation (Figure 12) and by cell-penetrating peptides (CPPs) (Figure 13) and. In both approaches, the goal was to assess cytotoxicity and transfection efficiency, and to optimize parameters for use in future experiments.

Under a collaboration agreement with Trince Bio, photoporation using a LumiPore device prototype was evaluated in iPSCs to assess cell death and efficiency of cargo uptake. Two different laser intensities were used in the experiment, E40 and E80, with E80 being the stronger setting and representing 80% of the laser's total capacity. Four different 2-fold dilutions of the LS2-C nanosensitiser molecule were tested, ranging from 1:6.25 to 1:50, and Transfection efficiency was assessed by counting the cells with the green signal of the fluorescent cargo, FITC-Dextran, and dividing them by the total number of cells in the picture.

Results demonstrated lower cell survival when using the most concentrated nanosensitiser conditions (1:6.25) at both laser intensities, with cell confluency percentages of approximately 1.2% for E40 and 0.86% for E80. In contrast, the other dilutions resulted in cell confluences above 5%. The experiment was carried out in a 96-well plate, and 25,000 iPSCs were seeded per well.

The E80 laser setting showed the highest cell confluency at a 1:12.5 nanosensitiser dilution, whereas E40 showed the highest confluency at a 1:25 dilution. Transfection efficiency was highest with E80 at a cargo dilution of 1:25, achieving 21.65%. Although this was the highest efficiency obtained using photoporation, it was lower than the efficiencies achieved with cell-penetrating peptides (see below) or Lipofectamine, which showed transfection efficiencies above 50%.

A. Transfection mediated photoporation and FITC-Dextran

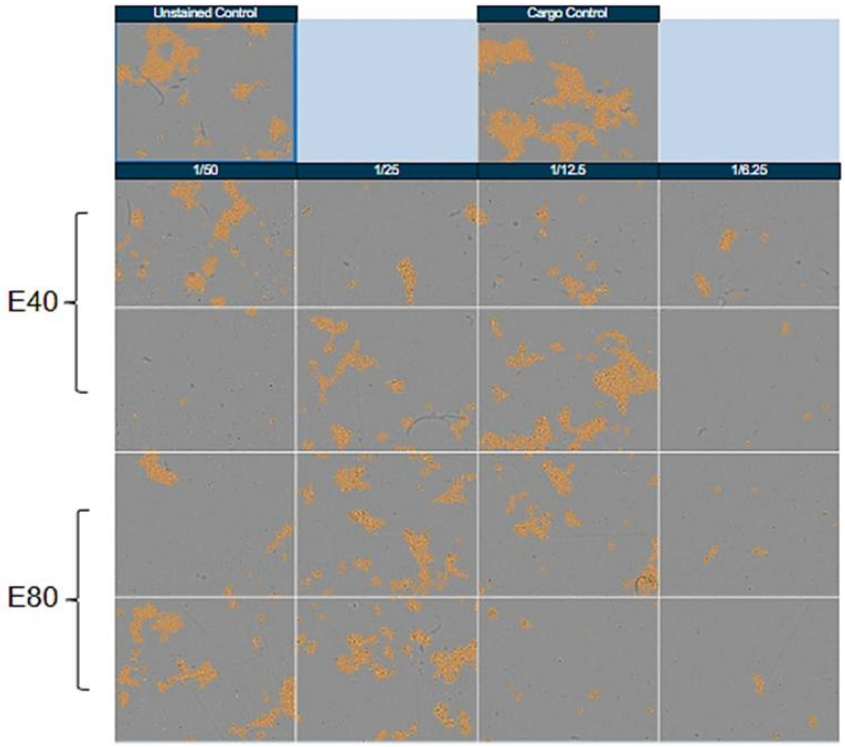

B. Fluorescent cargo and iPSCs

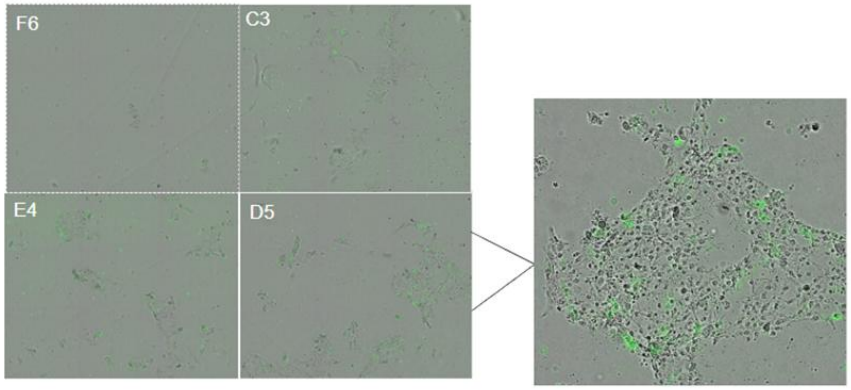

C.

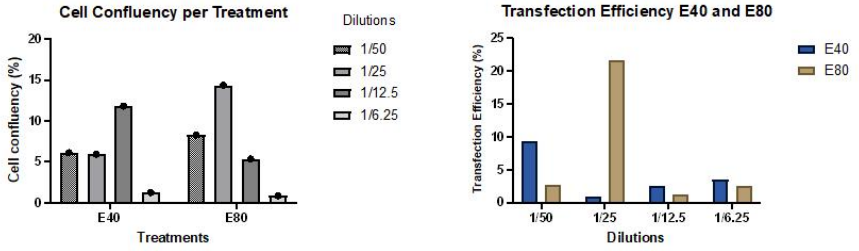

Figure 12. Photoporation of FITC-Dextran nanoparticles into iPSC.

A) Pseudocoloured (yellow) bright-field images of iPSC transfected via photoporation with FITC-Dextran cargo and LS2-C nanoparticles, using different concentrations of nanosensitizers and laser intensities. Two laser intensities (E40 and E80) were tested, under 4x 2-fold dilutions (1:6.25 – 1:50) of the LC2-C sensitiser nanoparticles. B) Representative enlarged images of cells photoporated with FITC-Dextran cargo (green signals), demonstrating loss of iPSC colony compaction and peeling from the culture surfaces.. C) Cell confluency and transfection efficiency for each laser intensity and nanosensitiser dilution tested, measured using image-based approaches outlined in section 3.12.

4.9 Cargo delivery to iPSC via Cell Penetrating Peptides (CPPs)

Transfection using CPPs was evaluated with four peptides, all labelled with Fluorescein amidites (FAM) dye: Arg9, a highly cationic peptide composed of 9 arginine residues; CPP9, a short arginine-rich peptide; TAT, a peptide derived from HIV-1; and TP10, a synthetic transportan derivative. A negative control was also included to assess the effects of the diluent on cell confluency. Six different 2-fold peptide dilutions were tested during transfection, ranging from 0.625 µM to 20 µM for each peptide. Twenty-four hours post-transfection, peptides were removed, cells were fixed, stained with DAPI, and visualised under fluorescence microscopy. Among the FAM labelled CPPs, Arg9 and CPP10 uptake reached up to ~30%. (Figure 13). According to the results, the most optimal concentrations for the peptides were between 2.5 µM and 10 µM, where confluence was between 5.04% and 27.65%. The highest concentration tested (20 µM) was toxic and decreased cell confluency in all cases. The peptides showing the greatest cytotoxicity were TAT and TP10, which, at

concentrations above 5 µM, caused significant cell death, with confluency percentages of 0.81% at 10 µM and 1.5% at 20 µM.

In terms of transfection efficiency, as expected, lower confluency percentages corresponded to higher transfection efficiency. TP10, the peptide that showed the most toxicity at the highest concentrations (1.5%), was found to have the highest transfection efficiency at these higher concentrations (77%). Arg9 and CPP10 showed higher transfection efficiency than TAT. Transfection efficiency was typically higher at concentrations of 5 µM or above. In addition, the absence of fluorescent signals in the negative control confirmed that there was no cross-contamination between treatments. However, noticeable cell death in the negative control suggests that the seeding technique could be further optimized. Overall, Arg9 and CPP10 exhibited lower cell toxicity and higher transfection efficiency at concentrations above 5 µM, while the lowest concentration (0.625 µM) and the highest concentration (20 µM), which could reduce transfection efficiency or cause excessive cell death would be avoided in future experiments. Importantly, compact colony morphology and cell adhesion were preserved under optimal Arg9 and CPP9 concentrations, and fluorescence detection pattern was uniform within the iPSC cytoplasm (Figure 13D). This reliably indicated uptake of peptides by iPSC.

A.

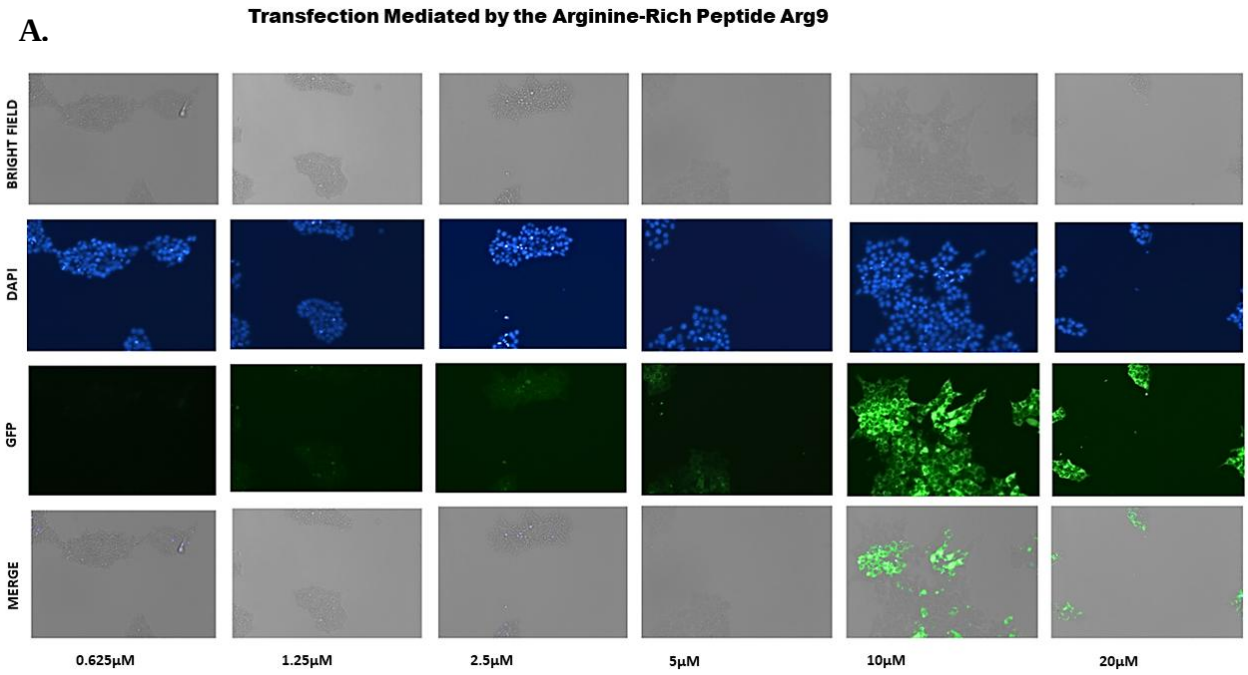
Transfection Mediated by the Arginine-Rich Peptide Arg9
BRIGHT FIELD
DAPI
GFP
MERGE
0.625µM
1.25µM
2.5µM
5µM
10µM
20µM

B.

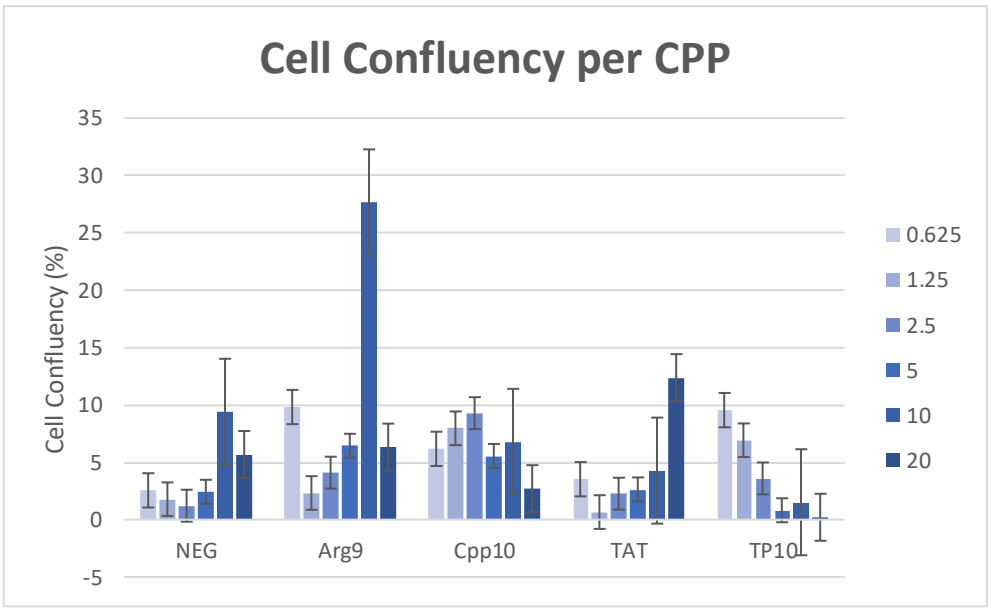
Cell Confluency per CPP
Cell Confluency (%)
35
30
25
20
15
10
5
0
-5
NEG
Arg9
Cpp10
TAT
TP10
0.625
1.25
2.5
5
10
20

C.

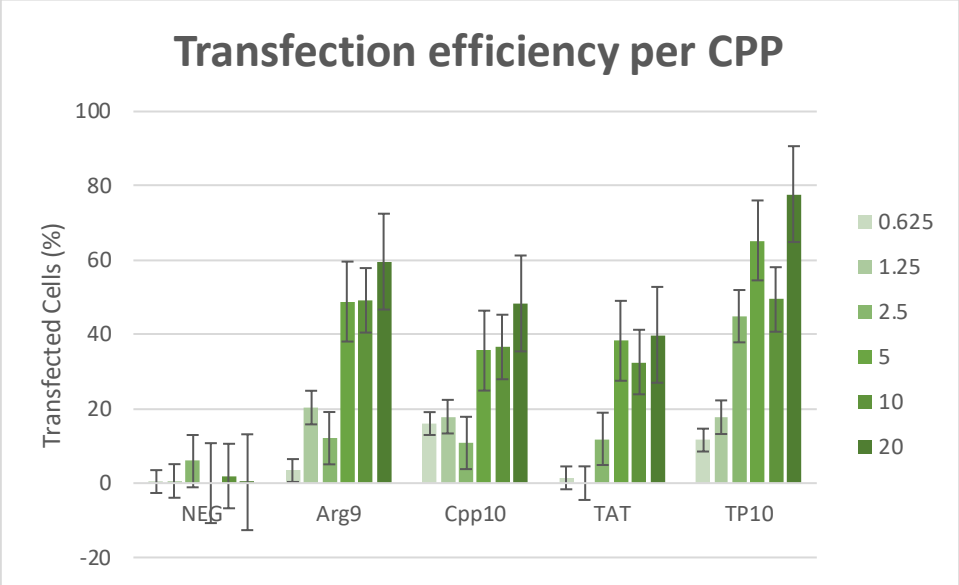

ANOVA

Source of Variation	*SS*	*df*	*MS*	*F*	*P-value*	*F crit*
Rows	6176.000808	5	1235.200162	9.179821874	0.000115936	2.710889837
Columns	6045.702472	4	1511.425618	11.23268793	6.08849E-05	2.866081402
Error	2691.120108	20	134.5560054			
Total	14912.82339	29				

D.

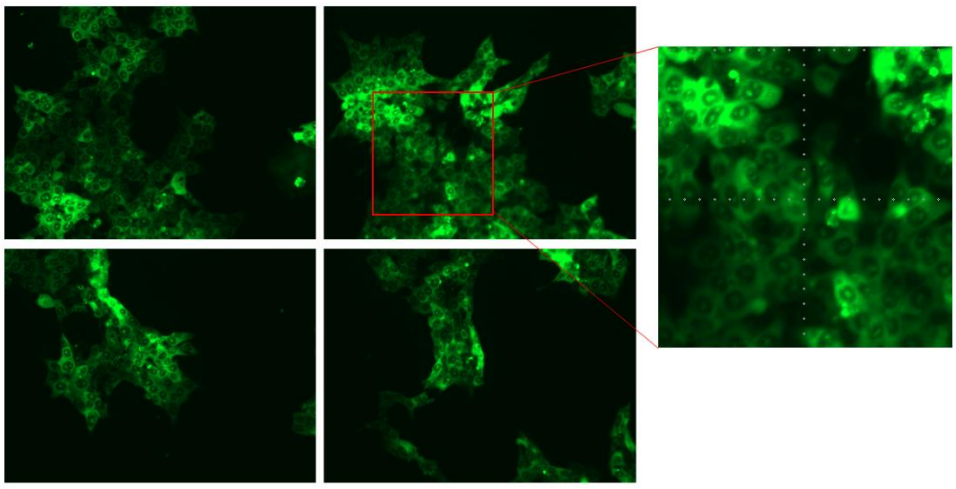

Figure 13. Transfection mediated via cell-penetrating peptides.

A) Representative images of iPSCs transfected with the Arg9 peptide at concentrations ranging from 0.625 µM to 20 µM. Brightfield, DAPI (nuclear staining, blue), GFP (FAM dye, green), and merged channels are shown. B) Quantification of percentage cell confluency for each cell-penetrating peptide (CPP), each used across a concentration range of 0.625–20 µM. The Standard Error is shown as a measure of variability. C) Transfection efficiency (%) for each CPP across a concentration range (0.625–20µM). The Standard Error is shown as a measure of variability. A total of 9 photos were analysed per condition, and an ANOVA two ways was carried out showing differences among concentrations and CPPs. D) Arg9 (10µM) cell images, demonstrating that the FAM-labelled peptide was localised in the cytoplasm of iPSCs.

5. Discussion

iPSCs have contributed substantially to advances in cell-based therapies. Their pluripotency, defined as the ability to differentiate into any somatic cell type of the human body, combined with their theoretically unlimited proliferative potential, has established them as a critical cellular source for regenerative medicine, drug discovery, disease modelling, and immunotherapy research. This project aimed to optimize and standardize culture conditions for the iPSC line SCTi003-A under defined settings and to evaluate different transfection strategies in this line, with the objective of generating hypoimmune cell variants suitable for future applications in immunotherapy and regenerative medicine.

In this study, cells were cultivated under xeno-free and feeder-free conditions to preserve genomic stability, maintain an undifferentiated phenotype, and sustain proliferative capacity. The use of mTeSR Plus medium for iPSC culture resulted in a morphological phenotype similar to the reported human embryonic stem cell (hESC) morphology (Haase et al., 2026).

The rationale for using this type of medium was to adapt the culture system toward Good Manufacturing Practice (GMP) compliance for future research, enabling the scalable production of cell products and reducing variability between clones. Throughout this research, feeder cells and xenogeneic components were avoided, as these can negatively affect culture quality and safety by promoting genomic instability, increasing batch-to-batch variability, and elevating the risk of spontaneous or undesired differentiation (Chaudhary & Villa-Diaz, 2025). Some components of mTeSR Plus remain proprietary due to company privacy policies from STEMCELL Technologies. However, its formulation is based on mTeSR™1, for which some components have been previously defined. Key components of this medium include FGF2, TGF-β, lithium, GABA, nutrients, and the xeno-derived additive BSA (Chaudhary & Villa-Diaz, 2025). In different studies, most of these components have been associated with cell proliferation and maintenance of the pluripotent state. For example, FGF2 binds to FGFR1 and FGFR4, and can also interact with ERBB3 and ERBB4, activating signalling pathways such as PI3K/AKT/mTOR and MAPK/ERK, which are well known for promoting cell proliferation. In contrast, TGF-β signals through TGFBR1/2 and/or ACVR1B/2A/2B receptors, activating the TGF-β signalling pathway, which is closely associated with adult and stem cell fate regulation (Kuo et al., 2020; Mullen & Wrana, 2017).

The mTeSR Plus medium used in this study allowed optimal culture performance in terms of colony morphology, cell density, and passaging frequency, enabling standardization of the process in the laboratory with a five-day passaging schedule and daily medium changes. However, no additional analyses were performed to further characterize the cells at the molecular or cytogenetic level. For example, G-banding or qPCR-based karyotyping was not conducted, nor were pluripotency markers such as OCT4, NANOG, SSEA4, and TRA-1-60 assessed by flow cytometry or other methods. Nevertheless, previous studies have shown that under xeno-free and feeder-free conditions, human pluripotent stem cells (hPSCs) can maintain these characteristics in approximately 90% of cells when cultured in mTeSR medium (Shimizu et al., 2022). Additionally, parallel studies performed by other students in

our lab demonstrated >90% pluripotency marker expression (OCT4, SOX2, TRA-1-81) and normal diploid karyotype in iPSC cultured under the same conditions (data not shown).

Regarding the cost of the culture medium, alternative formulations to mTeSR Plus could be considered in future studies. Several defined and more cost-effective media are currently available on the market and may represent suitable options to reduce production expenses while maintaining GMP compatibility for future cell therapy applications. Examples include Essential 8, TeSR-E8, ExCellerate, NutriStem, and HiDef B8 (P. Chen et al., 2025; Kuo et al., 2020; Lyra-Leite et al., 2022). Evaluating these alternatives could help optimize large-scale production processes and improve the economic feasibility of clinical-grade cell manufacturing.

After comparing Cultrex and Vitronectin XF coating matrices, a statistically significant difference was observed. However, that difference may have been influenced by measuring overconfluent areas on the well, which could have modified the outcome by adding outliers to the dataset. Acquisition of additional images across the wells could mitigate the outcome in future repeated studies. While Cultrex is a solubilized extracellular matrix preparation purified from the Engelbreth-Holm-Swarm (EHS) murine tumour and consists of a mixture of proteins, including laminin, collagen IV, entactin, and heparan sulfate proteoglycans (Biotechne, n.d.), Vitronectin XF is a well-defined glycoprotein present in the ECM. In our results, Cultrex supported faster cell proliferation, however, literature shows that in a similar comparison between Vitronectin XF and Matrigel, a membrane basal extract similar to Cultrex, significant differences in iPSC proliferation were not detected (Giles et al., 2025). Nevertheless, the use of Vitronectin XF is recommended for routine iPSC culture because it is a well-defined recombinant protein that mediates iPSC adhesion *via* αvβ5 integrins and has been shown to maintain self-renewal capacity under xeno-free conditions (Beers et al., 2012). For experiments involving substantial cellular stress (e.g., transfection), Cultrex was used instead because its basement-membrane–like matrix was considered more likely to

provide enhanced attachment and survival support for fragile iPSCs, reducing detachment and cell loss during manipulation. Future experiments can more deeply explore the effects of cell culture matrix on iPSC survival post-transfection, potentially introducing additional synthetic culture matrices such as Laminin-511 or Laminin-521 (Hagbard et al., 2018).

Optimizing cell culture conditions is not only essential to maintain the pluripotency and self-renewal properties of iPSCs, but also to prepare the cells for downstream applications without altering their biological responses. According to our transfection results, lipofection, a commonly used transfection method, achieved approximately 50% transfection efficiency, with almost no change in cell confluency compared to the control group, indicating low cytotoxicity. Some studies have reported lower toxicity when using Lipofectamine compared to other methods, as well as relatively low production costs (E. H. Kim et al., 2024). In other cell types, such as NK cells, transfection efficiencies ranging from 60% to 100% have been reported (Nakamura et al., 2016). However, when this method was used to deliver the CRISPR/Cas9 system into iPSCs, no gene knockouts were detected, suggesting that further optimization is required, such as annealing of a non-targeting crRNA to the tracr-ATTO RNA during optimisation, prolonging the RNP exposure time, and adapting the detection method abd/or incubation time to achieve efficient genome editing in the cell line used.

Additional approaches, such as cell-penetrating peptides (CPPs) and photoporation, can also be used to transfect iPSCs. Photoporation, marketed as a gentle technology for cargo delivery, was more cytotoxic than anticipated. This may be explained by the underlying mechanism of photoporation, in which gold nanosensitizers are exposed to a laser pulse, generating localized physicochemical effects such as transient heating, medium breakdown, surface plasmon resonance, and cavitation. These effects induce temporary micropores in the cell membrane, allowing exogenous molecules to enter the cell by diffusion. In cardiomyocytes, photoporation has been reported to achieve cell viability above 70% and transfection efficiencies of approximately 60% (Léger et al., 2024). For this to be translated

to iPSC with the same success, photoporation conditions may need to be further optimised. Optimisation avenues could include a recovery period of 3-6 hours between photoporation and medium change for removal of nanosensitiser and excess cargo. This would allow cells to adjust following the stress induced by photoporation, and prevent the peeling observed in Figure 12. Additionally, photoporation could be performed in the presence of anti-apoptotic agents such as ROCK inhibitors (Rivera et al., 2020), or CloneR and CEPT commercial cocktails (Lyra-Leite et al., 2022), and with the use of novel, less cytotoxic nanosensitiser formulations more recently made available to the iPSC Cell Therapies lab by Trince Bio through our collaborative agreement.

When testing iPSC transfection *via* CPPs, a considerable proportion of cells (up to 60%) were successfully transfected using the peptides Arg9 and CPP10, with high corresponding cellular viability and preservation of morphological characteristics. Some studies have also reported low toxicity associated with this method (Dey et al., 2017; Rádis-Baptista et al., 2017); however, this depends on several factors, such as the specific CPP used, its length, the nature of the cargo, the cell type, and the concentration applied (Dey et al., 2017). Cytotoxicity should be evaluated systematically, taking into account each of these variables independently.

While it is known that CPP cellular uptake is facilitated by endocytosis (clathrin-, caveolin-mediated, macropinocytosis), the exact mechanism by which these peptides enable nuclear delivery is not fully understood (Moon et al., 2019). Nevertheless, the versatility of this method makes it suitable for delivering not only the CRISPR/Cas9 system but also a variety of exogenous molecules, including nucleic acids and proteins (Rádis-Baptista et al., 2017). CPPs have already progressed to clinical evaluation, where they have been used to deliver a variety of therapeutic cargos in human trials (Gori et al., 2023). Additionally, their synthetic, modular nature and compatibility with serum-free, suspension cultures also make CPP-cargo formats amenable to controlled, scalable manufacturing in stirred-tank

bioreactors, a favourable attribute for use in allogeneic cell therapy manufacturing workflows.

In this study, no functional cargo was tested, only fluorescently-tagged CPPs. Therefore, future experiments could include delivering the CRISPR/Cas9 system using a CPP and subsequently assessing transfection efficiency and cell confluency. For this, a CPP-Cas9 fusion protein would need to be synthesised and tested, where the protein would be functionalized with a maleimide group (Ramakrishna et al., 2014), introduced *via* a small linker (e.g., a cysteine residue), as indicated below in the example of an Arg9-Cas9 fusion protein, where the Cas9 protein also incorporates two nuclear localisation signals (NLS), one at the N-terminus (c-Myc NLS; PKKKRKV) and one at the C-terminus (SV40 NLS; PPKKKRKL) (Feldan Therapeutics, 2025).

FAM–$(Arg)_9$–c- PKKKRKV–[C(Cas9)]–PPKKKRKL

Overall, CPPs represent promising alternatives to lipofection, electroporation, photoporation or other known methods for the delivery of genome-editing tools and other biomolecules into iPSCs, although further experimentation is needed to maximise uptake and cell survival, and assess functional knock-out outcomes. Alternative CPP formulations and delivery systems to achieve gene knockout, such as viral vectors, could also be considered in future studies; however, the associated mutational risks should be taken into account for the latter.

Some limitations of this study were related to the comparison between transfection methods, as different experimental conditions were used, including variations in the cargo molecules and the experiment scale. These differences may have limited the ability to directly compare the efficiency and cytotoxicity of each method under equivalent conditions. Additionally, further cell-based assays, such as G-banding, qPCR, or flow cytometry, could have been

included to assess potential genomic aberrations and the expression of pluripotency markers before and after transfection. This would have helped ensure that essential iPSC characteristics were not adversely affected by the transfection procedures, passaging, or cryopreservation. It is also important to note that transfection efficiency in this study was mainly measured through fluorescent microscopy. While this is a simple and rapid method, it can be difficult to clearly distinguish signals originating from outside versus inside the cells. Some of the aforementioned methods, such as qPCR, flow cytometry, or plasmid reporter systems, could also be appropriate for assessing transfection efficiency, as they provide more direct and quantitative measurements (Table 7). Future studies could emphasize direct comparisons between these methods and electroporation under standardized experimental conditions. However, due to cost and time constraints, transfection efficiency in this project was only assessed using fluorescent microscopy.

Table 7. Comparison of selected methods for the assessment of transfection efficiency. Adapted from Chong et al., (2021).

	Fluorescence microscopy	***Real-time PCR (qPCR)***	***Flow cytometry***
Description	Use of fluorescently tagged molecules to confirm transfection has taken place	Directly measures the expression level of nucleic acids post-transfection	Quantify the number of fluorescently labelled transfected cells
Quantitative or qualitative findings	Qualitative or semi-quantitative	Quantitative	Quantitative
Advantages	Easy and fast	Allows quantification of the transfection efficiency	Allows quantification of the transfection efficiency
Disadvantages	Inability to distinguish signals originating from interior vs exterior of cells	Expensive and laborious especially when testing multiple conditions and in transient transfection where regular monitoring of the transfection efficiency is needed	Expensive and more technically laborious

Additionally, different strategies for generating hypoimmune iPSCs could be explored in the future. For example, combining the knockout (KO) of B2M and CIITA with the expression of an HLA-E/B2M fusion protein, and introducing inhibitory molecules such as CD47 to prevent NK cell–mediated lysis. Genomic integrity should therefore be assessed through karyotyping or NGS analysis of crucial genes and pluripotency markers.

This study explored how the culture of iPSCs can be optimized for passaging and expansion conditions. In addition, evaluation was performed for Lipofection-based approaches to achieve genome editing of beta-2 microglobulin (B2M), a crucial component of MHC class I, and CIITA (Class II Major Histocompatibility Complex Transactivator), the master regulator of MHC class II molecule expression. Two additional transfection approaches, cell-penetrating peptides (CPPs) and photoporation, were also investigated and compared. While gene knockout was not yet achieved, the results highlight several promising avenues for optimisation, including the choice and properties of nanosensitizers for photoporation, the design of CPPs, and the tuning of cargo delivery conditions. Further work will also explore alternative crRNA sequences, protein instead of gDNA detection, as well as alternative hypoimmune engineering strategies and, once editing is successful, expanded assessments of cell viability, pluripotency and self-renewal to ensure that editing does not compromise iPSC quality. Notably, CPP-mediated delivery demonstrated efficient cellular uptake, as evidenced by fluorescence signal localisation and morphology within cells, and future experiments will focus on CPP–Cas9 fusion proteins to achieve precise knockout/knock-in hypoimmune edits.

6. Acknowledgements

In life, colleagues evolve into friends.
Guiding figures become true mentors.
Unfamiliar faces quietly become family.
And family endures, unchanged, even from afar.
I extend my sincere gratitude to each of you.

7. Bibliography

Aboul-Soud, M. A. M., Alzahrani, A. J., & Mahmoud, A. (2021). Induced Pluripotent Stem Cells (iPSCs)—Roles in Regenerative Therapies, Disease Modelling and Drug Screening. *Cells*, *10*(9), 2319. https://doi.org/10.3390/cells10092319

Adli, M. (2018). The CRISPR tool kit for genome editing and beyond. *Nature Communications*, *9*(1), 1911. https://doi.org/10.1038/s41467-018-04252-2

Aguirre, M., Escobar, M., Forero Amézquita, S., Cubillos, D., Rincón, C., Vanegas, P., Tarazona, M. P., Atuesta Escobar, S., Blanco, J. C., & Celis, L. G. (2023). Application of the Yamanaka Transcription Factors Oct4, Sox2, Klf4, and c-Myc from the Laboratory to the Clinic. *Genes*, *14*(9), 1697. https://doi.org/10.3390/genes14091697

Alali, Z., Ferdous, U. T., Nzila, A., Easmin, F., Shakoor, A., Zia, A. W., & Uddin, S. (2025). Stem Cell for Cancer Immunotherapy: Current Approaches and Challenges. *Stem Cell Reviews and Reports*, *21*(7), 1931–1954. https://doi.org/10.1007/s12015-025-10933-5

An, Z., Liu, P., Zheng, J., Si, C., Li, T., Chen, Y., Ma, T., Zhang, M. Q., Zhou, Q., & Ding, S. (2019). Sox2 and Klf4 as the Functional Core in Pluripotency Induction without Exogenous Oct4. *Cell Reports*, *29*(7), 1986-2000.e8. https://doi.org/10.1016/j.celrep.2019.10.026

Arrieta-Bolaños, E. (2025). Differential Alloreactivity: Lessons Learned From a Singular HLA Locus. *HLA*, *106*(6), e70489. https://doi.org/10.1111/tan.70489

Bae, S., Park, J., & Kim, J.-S. (2014). Cas-OFFinder: A fast and versatile algorithm that searches for potential off-target sites of Cas9 RNA-guided endonucleases. *Bioinformatics*, *30*(10), 1473–1475. https://doi.org/10.1093/bioinformatics/btu048

Beers, J., Gulbranson, D. R., George, N., Siniscalchi, L. I., Jones, J., Thomson, J. A., & Chen, G. (2012). Passaging and colony expansion of human pluripotent stem cells by enzyme-free dissociation in chemically defined culture conditions. *Nature Protocols*, *7*(11), 2029–2040. https://doi.org/10.1038/nprot.2012.130

Bendixen, L., Jensen, T. I., & Bak, R. O. (2023). CRISPR-Cas-mediated transcriptional modulation: The therapeutic promises of CRISPRa and CRISPRi. *Molecular Therapy*, *31*(7), 1920–1937. https://doi.org/10.1016/j.ymthe.2023.03.024

Biotechne. (n.d.). *Extracellular Matrix Proteins for Cell Culture Research Applications*. Retrieved February 22, 2026, from https://www.bio-techne.com/reagents/cell-culture-reagents/cultrex-bme-and-ecm-proteins

Bisht, D., Salave, S., Desai, N., Gogoi, P., Rana, D., Biswal, P., Sarma, G., Benival, D., Kommineni, N., & Desai, D. (2024). Genome editing and its role in vaccine, diagnosis, and therapeutic advancement. *International Journal of Biological Macromolecules*, *269*, 131802. https://doi.org/10.1016/j.ijbiomac.2024.131802

Bogomiakova, M. E., Bogomazova, A. N., & Lagarkova, M. A. (2024). Dysregulation of Immune Tolerance to Autologous iPSCs and Their Differentiated Derivatives. *Biochemistry (Moscow)*, *89*(5), 799–816. https://doi.org/10.1134/S0006297924050031

Brooks, I. R., Sheriff, A., Moran, D., Wang, J., & Jacków, J. (2023). Challenges of Gene Editing Therapies for Genodermatoses. *International Journal of Molecular Sciences*, *24*(3), 2298. https://doi.org/10.3390/ijms24032298

Cai, R., Lv, R., Shi, X., Yang, G., & Jin, J. (2023). CRISPR/dCas9 Tools: Epigenetic Mechanism and Application in Gene Transcriptional Regulation. *International Journal of Molecular Sciences*, *24*(19), 14865. https://doi.org/10.3390/ijms241914865

Campbell, K. H., McWhir, J., Ritchie, W. A., & Wilmut, I. (1996). Sheep cloned by nuclear transfer from a cultured cell line. *Nature*, *380*(6569), 64–66. https://doi.org/10.1038/380064a0

Cao, M.-L., Han, R.-Y., Chen, S.-D., Zhao, D.-Y., Shi, M.-Y., Zou, J.-H., Li, L., & Jiang, H.-K. (2025). Gene Editing: An Effective Tool for the Future Treatment of Kidney Disease. *Journal of Inflammation Research*, *Volume 18*, 4001–4018. https://doi.org/10.2147/JIR.S506760

Cardiff, R. A. L., Carothers, J. M., Zalatan, J. G., & Sauro, H. M. (2024). Systems-Level Modeling for CRISPR-Based Metabolic Engineering. *ACS Synthetic Biology*, *13*(9), 2643–2652. https://doi.org/10.1021/acssynbio.4c00053

Castro-Viñuelas, R., Sanjurjo-Rodríguez, C., Piñeiro-Ramil, M., Rodríguez-Fernández, S., López-Baltar, I., Fuentes-Boquete, I., Blanco, F. J., & Díaz-Prado, S. (2021). Tips and tricks for successfully culturing and adapting human induced pluripotent stem cells. *Molecular Therapy - Methods & Clinical Development*, *23*, 569–581. https://doi.org/10.1016/j.omtm.2021.10.013

Cerbini, T., Luo, Y., Rao, M. S., & Zou, J. (2015). Transfection, Selection, and Colony-picking of Human Induced Pluripotent Stem Cells TALEN-targeted with a GFP Gene into the AAVS1 Safe Harbor. *Journal of Visualized Experiments*, (96), 52504. https://doi.org/10.3791/52504

Chaaithanya, I. K., & Rajalingam, R. (2025). Emerging roles of natural killer cell ligands—HLA-E, HLA-F, HLA-G, MICA, and MICB—in in vitro fertilization outcomes. *Frontiers in Genetics*, *16*, 1661511. https://doi.org/10.3389/fgene.2025.1661511

Chadwick, A. C., & Musunuru, K. (2017). Genome Editing for the Study of Cardiovascular Diseases. *Current Cardiology Reports*, *19*(3), 22. https://doi.org/10.1007/s11886-017-0830-5

Chang, C.-Y., Ting, H.-C., Su, H.-L., & Jeng, J.-R. (2018). Combining Induced Pluripotent Stem Cells and Genome Editing Technologies for Clinical Applications. *Cell Transplantation*, *27*(3), 379–392. https://doi.org/10.1177/0963689718754560

Chaudhary, N., & Villa-Diaz, L. G. (2025). Advancements in the in vitro culture of human pluripotent stem cells: Progress, challenges, and future directions: comprehensive review. *Frontiers in Toxicology*, *7*, 1667573. https://doi.org/10.3389/ftox.2025.1667573

Chavez, J. C., Hoffmann, M. S., & Popplewell, L. L. (2025). Evaluating the Role of CAR-T Cell Therapy in the Context of Current Therapy Options for Patients With Relapsed or Refractory Follicular Lymphoma. *Transplantation and Cellular Therapy*, S2666636725012564. https://doi.org/10.1016/j.jtct.2025.06.013

Chen, P., Gao, J., Feng, J., Tao, H., Yu, Y., Li, Y., Liu, J., Lu, S., & Wang, W. (2025). The Application of iPSCs in Tumour Immunotherapy. *Expert Reviews in Molecular Medicine*, *27*, e26. https://doi.org/10.1017/erm.2025.10006

Chen, Y., Li, M., & Wu, Y. (2024). The occurrence and development of induced pluripotent stem cells. *Frontiers in Genetics*, *15*, 1389558. https://doi.org/10.3389/fgene.2024.1389558

Choi, I. Y., Lim, H. T., Che, Y. H., Lee, G., & Kim, Y. J. (2021). Inhibition of the Combinatorial Signaling of Transforming Growth Factor-Beta and NOTCH Promotes Myotube Formation of Human Pluripotent Stem Cell-Derived Skeletal Muscle Progenitor Cells. *Cells*, *10*(7), 1649. https://doi.org/10.3390/cells10071649

Chong, Z. X., Yeap, S. K., & Ho, W. Y. (2021a). Transfection types, methods and strategies: A technical review. *PeerJ*, *9*, e11165. https://doi.org/10.7717/peerj.11165

Chong, Z. X., Yeap, S. K., & Ho, W. Y. (2021b). Transfection types, methods and strategies: A technical review. *PeerJ*, *9*, e11165. https://doi.org/10.7717/peerj.11165

Christian, M., Cermak, T., Doyle, E. L., Schmidt, C., Zhang, F., Hummel, A., Bogdanove, A. J., & Voytas, D. F. (2010). Targeting DNA Double-Strand Breaks with TAL Effector Nucleases. *Genetics*, *186*(2), 757–761. https://doi.org/10.1534/genetics.110.120717

Cohen, R. N., Van Der Aa, M. A. E. M., Macaraeg, N., Lee, A. P., & Szoka, F. C. (2009). Quantification of plasmid DNA copies in the nucleus after lipoplex and polyplex transfection. *Journal of Controlled Release*, *135*(2), 166–174. https://doi.org/10.1016/j.jconrel.2008.12.016

Crew, M. D., Cannon, M. J., Phanavanh, B., & Garcia-Borges, C. N. (2005). An HLA-E single chain trimer inhibits human NK cell reactivity towards porcine cells. *Molecular Immunology*, *42*(10), 1205–1214. https://doi.org/10.1016/j.molimm.2004.11.013

Czerwińska, P., Mazurek, S., Kołodziejczak, I., & Wiznerowicz, M. (2019). Gene delivery methods and genome editing of human pluripotent stem cells. *Reports of Practical Oncology & Radiotherapy*, *24*(2), 180–187. https://doi.org/10.1016/j.rpor.2019.01.007

Damian, D. (2026). Human Leukocyte Antigen (HLA) and Tumor Immunity: A Critical Link in Cancer Immunotherapy. *Immunity, Inflammation and Disease*, *14*(2), e70363. https://doi.org/10.1002/iid3.70363

Dey, C., Narayan, G., Krishna Kumar, H., Borgohain, M., & Lenka, N. (2017). Cell-Penetrating Peptides as a Tool to Deliver Biologically Active Recombinant Proteins to Generate Transgene-Free Induced Pluripotent Stem Cells. *Studies on Stem Cells Research and Therapy*, *3*(1), 006–015. https://doi.org/10.17352/sscrt.000011

Dolenc, I. (2025). CD74 and Proteases: Impact of Location on Immune and Cellular Functions. *Cells*, *14*(24), 1960. https://doi.org/10.3390/cells14241960

Doss, M. X., & Sachinidis, A. (2019). Current Challenges of iPSC-Based Disease Modeling and Therapeutic Implications. *Cells*, *8*(5), 403. https://doi.org/10.3390/cells8050403

Dwivedi, A. K., Mahesh, A., Sanfeliu, A., Larkin, J., Siwicki, R. A., Sweeney, K. J., O'Brien, D. F., Widdess-Walsh, P., Picelli, S., Henshall, D. C., & Tiwari, V. K. (2025). High-resolution multimodal profiling of human epileptic brain activity via explanted depth electrodes. *JCI Insight*, *10*(1), e184518. https://doi.org/10.1172/jci.insight.184518

EditCo's. (2026). *Analysis tool can be referenced in the following way: ICE CRISPR Analysis.* https://editco.my.site.com/support/s/article/Citing-the-ICE-Analysis-Tool-in-a-Publication

El Semary, N. A. H., Fadiel, A., Eichenbaum, K. D., & Alhusayni, S. A. (2026). Prokaryotic Molecular Defense Mechanisms and Their Potential Applications in Cancer Biology: A Special Consideration for Cyanobacterial Systems. *Current Issues in Molecular Biology*, *48*(1), 105. https://doi.org/10.3390/cimb48010105

Fang, F., Xie, S., Chen, M., Li, Y., Yue, J., Ma, J., Shu, X., He, Y., Xiao, W., & Tian, Z. (2022). Advances in NK cell production. *Cellular & Molecular Immunology*, *19*(4), 460–481. https://doi.org/10.1038/s41423-021-00808-3

Fate Therapeutics, Inc. (2021). *Fate Therapeutics Announces Positive Interim Clinical Data from its FT596 and FT516 Off-the-shelf, iPSC-derived NK Cell Programs for B-cell*

Lymphoma. https://ir.fatetherapeutics.com/news-releases/news-release-details/fate-therapeutics-announces-positive-interim-clinical-data-its

Feldan Therapeutics. (2025). *Feldan Therapeutics*. https://www.feldan.com/about

Fiorini, E., Malinova, A., Schreyer, D., Pasini, D., Bevere, M., Alessio, G., Rosa, D., D'Agosto, S., Azzolin, L., Milite, S., Andreani, S., Lupo, F., Veghini, L., Grimaldi, S., Pedron, S., Castellucci, M., Nourse, C., Salvia, R., Malleo, G., … Corbo, V. (2025). MYC ecDNA promotes intratumour heterogeneity and plasticity in PDAC. *Nature*, *640*(8059), 811–820. https://doi.org/10.1038/s41586-025-08721-9

Freitas-Alves, N. S., Moreira-Pinto, C. E., Távora, F. T. P. K., Paes-de-Melo, B., Arraes, F. B. M., Lourenço-Tessutti, I. T., Moura, S. M., Oliveira, A. C., Morgante, C. V., Qi, Y., & Fatima Grossi-de-Sa, M. (2025). CRISPR/Cas genome editing in soybean: Challenges and new insights to overcome existing bottlenecks. *Journal of Advanced Research*, *73*, 53–72. https://doi.org/10.1016/j.jare.2024.08.024

Fus-Kujawa, A., Prus, P., Bajdak-Rusinek, K., Teper, P., Gawron, K., Kowalczuk, A., & Sieron, A. L. (2021). An Overview of Methods and Tools for Transfection of Eukaryotic Cells in vitro. *Frontiers in Bioengineering and Biotechnology*, *9*, 701031. https://doi.org/10.3389/fbioe.2021.701031

Gaj, T., Guo, J., Kato, Y., Sirk, S. J., & Barbas, C. F. (2012). Targeted gene knockout by direct delivery of zinc-finger nuclease proteins. *Nature Methods*, *9*(8), 805–807. https://doi.org/10.1038/nmeth.2030

Gao, F., Li, X., Xu, K., Wang, R., & Guan, X. (2023). C-MYC mediates the crosstalk between breast cancer cells and tumor microenvironment. *Cell Communication and Signaling*, *21*(1), 28. https://doi.org/10.1186/s12964-023-01043-1

Giles, R., Meijer, E. M., Maas, R. G. C., Van Dijk, C. G. M., Verhaar, M. C., & Cheng, C. (2025). Animal-free alternatives for Matrigel in human iPSC-derived blood vessel organoid culture. *Scientific Reports*, *15*(1), 36042. https://doi.org/10.1038/s41598-025-20091-w

Gori, A., Lodigiani, G., Colombarolli, S. G., Bergamaschi, G., & Vitali, A. (2023). Cell Penetrating Peptides: Classification, Mechanisms, Methods of Study, and Applications. *ChemMedChem*, *18*(17), e202300236. https://doi.org/10.1002/cmdc.202300236

Guan, J., Wang, G., Wang, J., Zhang, Z., Fu, Y., Cheng, L., Meng, G., Lyu, Y., Zhu, J., Li, Y., Wang, Y., Liuyang, S., Liu, B., Yang, Z., He, H., Zhong, X., Chen, Q., Zhang, X., Sun, S., … Deng, H. (2022). Chemical reprogramming of human somatic cells to pluripotent stem cells. *Nature*, *605*(7909), 325–331. https://doi.org/10.1038/s41586-022-04593-5

Guido, N., Starostina, E., Leake, D., & Saaem, I. (2016). Improved PCR Amplification of Broad Spectrum GC DNA Templates. *PLOS ONE*, *11*(6), e0156478. https://doi.org/10.1371/journal.pone.0156478

Guney, M., Hruba, P., & Viklicky, O. (2026). Molecular diagnostics in HLA-incompatible kidney transplantation. *Transplantation Reviews*, *40*(2), 101006. https://doi.org/10.1016/j.trre.2026.101006

Haase, A., Ruhparwar, A., & Martin, U. (2026). GMP-compliant manufacturing of iPSC-derived therapeutic cell products: Technologies, applications, risks and limitations. *Advanced Drug Delivery Reviews*, *229*, 115744. https://doi.org/10.1016/j.addr.2025.115744

Habib, O., Habib, G., Hwang, G.-H., & Bae, S. (2022). Comprehensive analysis of prime editing outcomes in human embryonic stem cells. *Nucleic Acids Research*, *50*(2), 1187–1197. https://doi.org/10.1093/nar/gkab1295

Hagbard, L., Cameron, K., August, P., Penton, C., Parmar, M., Hay, D. C., & Kallur, T. (2018). Developing defined substrates for stem cell culture and differentiation. *Philosophical Transactions of the Royal Society B: Biological Sciences*, *373*(1750), 20170230. https://doi.org/10.1098/rstb.2017.0230

Han, J. L., & Entcheva, E. (2023). Gene Modulation with CRISPR-based Tools in Human iPSC-Cardiomyocytes. *Stem Cell Reviews and Reports*, *19*(4), 886–905. https://doi.org/10.1007/s12015-023-10506-4

Han, J., Zhang, B., Zheng, S., Jiang, Y., Zhang, X., & Mao, K. (2024). The Progress and Prospects of Immune Cell Therapy for the Treatment of Cancer. *Cell Transplantation*, *33*, 09636897241231892. https://doi.org/10.1177/09636897241231892

Heeren, J. J. F. (2025). *Building tolerance: Employing genome engineering toward universal Treg therapy*. *117*(12).

Heinel, A. (2020). Pioneers of Crispr Gene Editing win Chemistry Nobel. *Nature*, 346.

Hong, Z., Zhao, Y., Pahlavan, S., Wang, X., Han, S., Wang, X., & Wang, K. (2025). iPSC modification strategies to induce immune tolerance. *Life Medicine*, *4*(3), lnaf016. https://doi.org/10.1093/lifemedi/lnaf016

Hu, S., Gan, M., Wei, Z., Shang, P., Song, L., Feng, J., Chen, L., Niu, L., Wang, Y., Zhang, S., Shen, L., Zhu, L., & Zhao, Y. (2024). Identification of host factors for livestock and poultry viruses: Genome-wide screening technology based on the CRISPR system. *Frontiers in Microbiology*, *15*, 1498641. https://doi.org/10.3389/fmicb.2024.1498641

Ingle, R. G., M. Elossaily, G., Ansari, M. N., & Makhijani, S. (2025). Unlocking the potential: Advancements and applications of gene therapy in severe disorders. *Annals of Medicine*, *57*(1), 2516697. https://doi.org/10.1080/07853890.2025.2516697

Integrated DNA Technologies. (2023). *Alt-RTM CRISPR-Cas9 System* [Protocol]. Integrated DNA Technologies, Inc. https://doi.org/RUO22-0670_002.1

Jordan, E. T., Collins, M., Terefe, J., Ugozzoli, L., & Rubio, T. (2008). *Optimizing Electroporation Conditions in Primary and Other Difficult-to-Transfect Cells*.

Kantor, A., McClements, M., & MacLaren, R. (2020). CRISPR-Cas9 DNA Base-Editing and Prime-Editing. *International Journal of Molecular Sciences*, *21*(17), 6240. https://doi.org/10.3390/ijms21176240

Karaoglu, I. C., Duymaz, D., Rashid, M. M., & Kizilel, S. (2025). Immune-evasive beta cells in type 1 diabetes: Innovations in genetic engineering, biomaterials, and computational modeling. *Frontiers in Immunology*, *16*, 1618086. https://doi.org/10.3389/fimmu.2025.1618086

Khan, N., Bammidi, S., Chattopadhyay, S., & Jayandharan, G. R. (2019). Combination Suicide Gene Delivery with an Adeno-Associated Virus Vector Encoding Inducible Caspase-9 and a Chemical Inducer of Dimerization Is Effective in a Xenotransplantation Model of Hepatocellular Carcinoma. *Bioconjugate Chemistry*, *30*(6), 1754–1762. https://doi.org/10.1021/acs.bioconjchem.9b00291

Kim, E. H., Teerdhala, S. V., Padilla, M. S., Joseph, R. A., Li, J. J., Haley, R. M., & Mitchell, M. J. (2024). Lipid nanoparticle-mediated RNA delivery for immune cell modulation. *European Journal of Immunology*, *54*(12), 2451008. https://doi.org/10.1002/eji.202451008

Kim, J. Y., Nam, Y., Rim, Y. A., & Ju, J. H. (2022). Review of the Current Trends in Clinical Trials Involving Induced Pluripotent Stem Cells. *Stem Cell Reviews and Reports*, *18*(1), 142–154. https://doi.org/10.1007/s12015-021-10262-3

Kimura, Y., Shofuda, T., Higuchi, Y., Nagamori, I., Oda, M., Nakamori, M., Onodera, M., Kanematsu, D., Yamamoto, A., Katsuma, A., Suemizu, H., Nakano, T., Kanemura, Y., & Mochizuki, H. (2019). Human Genomic Safe Harbors and the Suicide Gene-Based Safeguard System for iPSC-Based Cell Therapy. *Stem Cells Translational Medicine*, *8*(7), 627–638. https://doi.org/10.1002/sctm.18-0039

Kirkeby, A., Main, H., & Carpenter, M. (2025). Pluripotent stem-cell-derived therapies in clinical trial: A 2025 update. *Cell Stem Cell*, *32*(1), 10–37. https://doi.org/10.1016/j.stem.2024.12.005

Koblan, L. W., Erdos, M. R., Wilson, C., Cabral, W. A., Levy, J. M., Xiong, Z.-M., Tavarez, U. L., Davison, L. M., Gete, Y. G., Mao, X., Newby, G. A., Doherty, S. P., Narisu, N., Sheng, Q., Krilow, C., Lin, C. Y., Gordon, L. B., Cao, K., Collins, F. S., … Liu, D. R. (2021). In vivo base editing rescues Hutchinson–Gilford progeria syndrome in mice. *Nature*, *589*(7843), 608–614. https://doi.org/10.1038/s41586-020-03086-7

Koga, K., Wang, B., & Kaneko, S. (2020). Current status and future perspectives of HLA-edited induced pluripotent stem cells. *Inflammation and Regeneration*, *40*(1), 23. https://doi.org/10.1186/s41232-020-00132-9

Kress, T. R., Sabò, A., & Amati, B. (2015). MYC: Connecting selective transcriptional control to global RNA production. *Nature Reviews Cancer*, *15*(10), 593–607. https://doi.org/10.1038/nrc3984

Kuo, H.-H., Gao, X., DeKeyser, J.-M., Fetterman, K. A., Pinheiro, E. A., Weddle, C. J., Fonoudi, H., Orman, M. V., Romero-Tejeda, M., Jouni, M., Blancard, M., Magdy, T., Epting, C. L., George, A. L., & Burridge, P. W. (2020). Negligible-Cost and Weekend-Free Chemically Defined Human iPSC Culture. *Stem Cell Reports*, *14*(2), 256–270. https://doi.org/10.1016/j.stemcr.2019.12.007

Kwon, Y.-W., Ahn, H.-S., Lee, J.-W., Yang, H.-M., Cho, H.-J., Kim, S. J., Lee, S.-H., Yang, H.-M., Jang, H.-D., Kim, S. J., & Kim, H.-S. (2021). HLA DR Genome Editing with TALENs in Human iPSCs Produced Immune-Tolerant Dendritic Cells. *Stem Cells International*, *2021*, 1–14. https://doi.org/10.1155/2021/8873383

Li, Y.-R., Fang, Y., Niu, S., Chen, Y., Lyu, Z., & Yang, L. (2025). Managing allorejection in off-the-shelf CAR-engineered cell therapies. *Molecular Therapy*, *33*(6), 2368–2390. https://doi.org/10.1016/j.ymthe.2024.11.035

Liang, X., Potter, J., Kumar, S., Zou, Y., Quintanilla, R., Sridharan, M., Carte, J., Chen, W., Roark, N., Ranganathan, S., Ravinder, N., & Chesnut, J. D. (2015). Rapid and highly efficient mammalian cell engineering via Cas9 protein transfection. *Journal of Biotechnology*, *208*, 44–53. https://doi.org/10.1016/j.jbiotec.2015.04.024

Lim, W. A., & June, C. H. (2017). The Principles of Engineering Immune Cells to Treat Cancer. *Cell*, *168*(4), 724–740. https://doi.org/10.1016/j.cell.2017.01.016

Lipus, A., Janosz, E., Ackermann, M., Hetzel, M., Dahlke, J., Buchegger, T., Wunderlich, S., Martin, U., Cathomen, T., Schambach, A., Moritz, T., & Lachmann, N. (2020). Targeted Integration of Inducible Caspase-9 in Human iPSCs Allows Efficient in vitro Clearance of iPSCs and iPSC-Macrophages. *International Journal of Molecular Sciences*, *21*(7), 2481. https://doi.org/10.3390/ijms21072481

Liu, D., Cao, D., & Han, R. (2025). Recent advances in therapeutic gene-editing technologies. *Molecular Therapy*, *33*(6), 2619–2644. https://doi.org/10.1016/j.ymthe.2025.03.026

Liu, G., David, B. T., Trawczynski, M., & Fessler, R. G. (2020). Advances in Pluripotent Stem Cells: History, Mechanisms, Technologies, and Applications. *Stem Cell Reviews and Reports*, *16*(1), 3–32. https://doi.org/10.1007/s12015-019-09935-x

Lyra-Leite, D. M., Gutiérrez-Gutiérrez, Ó., Wang, M., Zhou, Y., Cyganek, L., & Burridge, P. W. (2022). A review of protocols for human iPSC culture, cardiac differentiation, subtype-specification, maturation, and direct reprogramming. *STAR Protocols*, *3*(3), 101560. https://doi.org/10.1016/j.xpro.2022.101560

Ma, M., Ge, J.-Y., Nie, Y.-Z., Li, Y.-M., & Zheng, Y.-W. (2024). Developing Humanized Animal Models with Transplantable Human iPSC-Derived Cells. *Frontiers in Bioscience-Landmark*, *29*(1), 34. https://doi.org/10.31083/j.fbl2901034

Mattapally, S., Pawlik, K. M., Fast, V. G., Zumaquero, E., Lund, F. E., Randall, T. D., Townes, T. M., & Zhang, J. (2018). Human Leukocyte Antigen Class I and II Knockout Human Induced Pluripotent Stem Cell–Derived Cells: Universal Donor for Cell Therapy. *Journal of the American Heart Association*, *7*(23), e010239. https://doi.org/10.1161/JAHA.118.010239

McGraw, E., Laurent, G. M., & Avila, L. A. (2024). Nanoparticle-Mediated Photoporation: Expanding Horizons in Drug Delivery. *Nanoscale Advances*, *6*(20), 5007–5019. https://doi.org/10.1039/D4NA00122B

Mishra, H. K., & Kalyuzhny, A. (2024). Revolutionizing Cancer Treatments through Stem Cell-Derived CAR T Cells for Immunotherapy: Opening New Horizons for the Future of Oncology. *Cells*, *13*(18), 1516. https://doi.org/10.3390/cells13181516

Modell, A. E., Lim, D., Nguyen, T. M., Sreekanth, V., & Choudhary, A. (2022). CRISPR-based therapeutics: Current challenges and future applications. *Trends in Pharmacological Sciences*, *43*(2), 151–161. https://doi.org/10.1016/j.tips.2021.10.012

Moriyama, H., & Yokota, T. (2025). Cardiac Cell and Animal Models for Duchenne Muscular Dystrophy in the Era of Gene Therapy and Precision Medicine. *Cells*, *14*(17), 1326. https://doi.org/10.3390/cells14171326

Mullen, A. C., & Wrana, J. L. (2017). TGF-β Family Signaling in Embryonic and Somatic Stem-Cell Renewal and Differentiation. *Cold Spring Harbor Perspectives in Biology*, *9*(7), a022186. https://doi.org/10.1101/cshperspect.a022186

Murugan, D., Murugesan, V., Panchapakesan, B., & Rangasamy, L. (2022). Nanoparticle Enhancement of Natural Killer (NK) Cell-Based Immunotherapy. *Cancers*, *14*(21), 5438. https://doi.org/10.3390/cancers14215438

Nakamura, T., Kuroi, M., Fujiwara, Y., Warashina, S., Sato, Y., & Harashima, H. (2016). Small-sized, stable lipid nanoparticle for the efficient delivery of siRNA to human immune cell lines. *Scientific Reports*, *6*(1), 37849. https://doi.org/10.1038/srep37849

Nikcevic, G., Kovacevic-Grujicic, N., & Stevanovic, M. (2003). Improved transfection efficiency of cultured human cells. *Cell Biology International*, *27*(9), 735–737. https://doi.org/10.1016/S1065-6995(03)00143-4

Park, J., Kim, J., Shin, B., Schler, H. R., Kim, J., & Kim, K.-P. (2024). Inducing Pluripotency in Somatic Cells: Historical Perspective and Recent Advances. *International Journal of Stem Cells*, *17*(4), 363–373. https://doi.org/10.15283/ijsc23148

Poetsch, M. S., Strano, A., & Guan, K. (2022). Human Induced Pluripotent Stem Cells: From Cell Origin, Genomic Stability, and Epigenetic Memory to Translational Medicine. *Stem Cells*, *40*(6), 546–555. https://doi.org/10.1093/stmcls/sxac020

Przymuszała, M., Białobrzeska, M., Dulak, J., & Florczyk-Soluch, U. (2026). Current Trends in Duchenne Muscular Dystrophy Research and Therapy: 3D Cardiac Modelling. *Journal of Cachexia, Sarcopenia and Muscle*, *17*(1), e70180. https://doi.org/10.1002/jcsm.70180

Rádis-Baptista, G., Campelo, I. S., Morlighem, J.-É. R. L., Melo, L. M., & Freitas, V. J. F. (2017). Cell-penetrating peptides (CPPs): From delivery of nucleic acids and antigens to transduction of engineered nucleases for application in transgenesis. *Journal of Biotechnology*, *252*, 15–26. https://doi.org/10.1016/j.jbiotec.2017.05.002

Ramakrishna, S., Kwaku Dad, A.-B., Beloor, J., Gopalappa, R., Lee, S.-K., & Kim, H. (2014). Gene disruption by cell-penetrating peptide-mediated delivery of Cas9 protein and guide RNA. *Genome Research*, *24*(6), 1020–1027. https://doi.org/10.1101/gr.171264.113

Ramirez-Phillips, A. C., & Liu, D. (2021). Therapeutic Genome Editing and In Vivo Delivery. *The AAPS Journal*, *23*(4), 80. https://doi.org/10.1208/s12248-021-00613-w

Razavi, Z., Soltani, M., Souri, M., & Van Wijnen, A. J. (2024). CRISPR innovations in tissue engineering and gene editing. *Life Sciences*, *358*, 123120. https://doi.org/10.1016/j.lfs.2024.123120

R&D Systems. (n.d.). *Extracellular Matrices & Cell Culture Products* |. Retrieved March 21, 2026, from https://www.rndsystems.com/products/cell-culture/cultrex/bme

Rivera, T., Zhao, Y., Ni, Y., & Wang, J. (2020). Human-Induced Pluripotent Stem Cell Culture Methods Under cGMP Conditions. *Current Protocols in Stem Cell Biology*, *54*(1), e117. https://doi.org/10.1002/cpsc.117

Saha, S. K., Saikot, F. K., Rahman, Md. S., Jamal, M. A. H. M., Rahman, S. M. K., Islam, S. M. R., & Kim, K.-H. (2019). Programmable Molecular Scissors: Applications of a New Tool for Genome Editing in Biotech. *Molecular Therapy Nucleic Acids*, *14*, 212–238. https://doi.org/10.1016/j.omtn.2018.11.016

Seimetz, D., Heller, K., & Richter, J. (2019). Approval of First CAR-Ts: Have we Solved all Hurdles for ATMPs? *Cell Medicine*, *11*, 2155179018822781. https://doi.org/10.1177/2155179018822781

Shen, Q., Ruan, H., Zhang, H., Wu, T., Zhu, K., Han, W., Dong, R., Ming, T., Qi, H., & Zhang, Y. (2024). Utilization of CRISPR-Cas genome editing technology in filamentous fungi: Function and advancement potentiality. *Frontiers in Microbiology*, *15*, 1375120. https://doi.org/10.3389/fmicb.2024.1375120

Shi, X., Zhang, K., Yu, F., Qi, Q., Cai, X., & Zhang, Y. (2024). Advancements and Innovative Strategies in Induced Pluripotent Stem Cell-Derived Mesenchymal Stem Cell Therapy: A Comprehensive Review. *Stem Cells International*, *2024*(1), 4073485. https://doi.org/10.1155/2024/4073485

Shimizu, E., Iguchi, H., Le, M. N. T., Nakamura, Y., Kobayashi, D., Arai, Y., Takakura, K., Benno, S., Yoshida, N., Tsukahara, M., Haneda, S., & Hasegawa, K. (2022). A chemically-defined plastic scaffold for the xeno-free production of human pluripotent stem cells. *Scientific Reports*, *12*(1), 2516. https://doi.org/10.1038/s41598-022-06356-8

STEMCELL Technologies. (n.d.). *Vitronectin XF™ Matrix for Pluripotent Stem Cell Culture* |. Retrieved March 21, 2026, from https://www.stemcell.com/products/vitronectin-xf.html

Sung, C. K., & Yim, H. (2020). CRISPR-mediated promoter de/methylation technologies for gene regulation. *Archives of Pharmacal Research*, *43*(7), 705–713. https://doi.org/10.1007/s12272-020-01257-8

Takahashi, K., Tanabe, K., Ohnuki, M., Narita, M., Ichisaka, T., Tomoda, K., & Yamanaka, S. (2007). Induction of Pluripotent Stem Cells from Adult Human Fibroblasts by Defined Factors. *Cell*, *131*(5), 861–872. https://doi.org/10.1016/j.cell.2007.11.019

Takahashi, K., & Yamanaka, S. (2006). Induction of Pluripotent Stem Cells from Mouse Embryonic and Adult Fibroblast Cultures by Defined Factors. *Cell*, *126*(4), 663–676. https://doi.org/10.1016/j.cell.2006.07.024

Takahashi, K., & Yamanaka, S. (2016). A decade of transcription factor-mediated reprogramming to pluripotency. *Nature Reviews Molecular Cell Biology*, *17*(3), 183–193. https://doi.org/10.1038/nrm.2016.8

Tan, S., Tao, Z., Loo, S., Su, L., Chen, X., & Ye, L. (2019). Non-viral vector based gene transfection with human induced pluripotent stem cells derived cardiomyocytes. *Scientific Reports*, *9*(1), 14404. https://doi.org/10.1038/s41598-019-50980-w

ThermoFisher Scientific. (2018). *Lipofectamine CRISPRMAX Transfection Reagent* [Protocol]. Thermo Fisher Scientific Inc. thermofisher.com/support.

Thomson, J. A., Itskovitz-Eldor, J., Shapiro, S. S., Waknitz, M. A., Swiergiel, J. J., Marshall, V. S., & Jones, J. M. (1998). Embryonic Stem Cell Lines Derived from Human Blastocysts. *Science*, *282*(5391), 1145–1147. https://doi.org/10.1126/science.282.5391.1145

Till, J. E., & McCulloch, E. A. (1961). A Direct Measurement of the Radiation Sensitivity of Normal Mouse Bone Marrow Cells. *Radiation Research*, *178*(2), 213–221. https://doi.org/10.1667/rrav01.1

Tizhoosh, H. R. (2005). Image thresholding using type II fuzzy sets. *Pattern Recognition*, *38*(12), 2363–2372. https://doi.org/10.1016/j.patcog.2005.02.014

Wang, G., Heimendinger, P., Ramelmeier, R. A., & Wang, W. (2022). Pluripotent stem cell-based cell therapies: Current applications and future prospects. *Current Opinion in Biomedical Engineering*, *22*, 100390. https://doi.org/10.1016/j.cobme.2022.100390

Yu, J., Vodyanik, M. A., Smuga-Otto, K., Antosiewicz-Bourget, J., Frane, J. L., Tian, S., Nie, J., Jonsdottir, G. A., Ruotti, V., Stewart, R., Slukvin, I. I., & Thomson, J. A. (2007). Induced Pluripotent Stem Cell Lines Derived from Human Somatic Cells. *Science*, *318*(5858), 1917–1920. https://doi.org/10.1126/science.1151526

Yu, X., Liang, X., Xie, H., Kumar, S., Ravinder, N., Potter, J., De Mollerat Du Jeu, X., & Chesnut, J. D. (2016). Improved delivery of Cas9 protein/gRNA complexes using lipofectamine CRISPRMAX. *Biotechnology Letters*, *38*(6), 919–929. https://doi.org/10.1007/s10529-016-2064-9

Yuan, J., Ma, Y., Huang, T., Chen, Y., Peng, Y., Li, B., Li, J., Zhang, Y., Song, B., Sun, X., Ding, Q., Song, Y., & Chang, X. (2018). Genetic Modulation of RNA Splicing with a CRISPR-Guided Cytidine Deaminase. *Molecular Cell*, *72*(2), 380-394.e7. https://doi.org/10.1016/j.molcel.2018.09.002

Zakrzewski, W., Dobrzyński, M., Szymonowicz, M., & Rybak, Z. (2019). Stem cells: Past, present, and future. *Stem Cell Research & Therapy*, *10*(1), 68. https://doi.org/10.1186/s13287-019-1165-5

Zhang, J., Jia, Z., Pan, H., Ma, W., Liu, Y., Tian, X., Han, Y., Wang, Q., Zhou, C., & Zhang, J. (2025). From induced pluripotent stem cell (iPSC) to universal immune cells: Literature review of advances in a new generation of tumor therapies. *Translational Cancer Research*, *14*(4), 2495–2507. https://doi.org/10.21037/tcr-24-1087

Zhou, H., Ye, P., Xiong, W., Duan, X., Jing, S., He, Y., Zeng, Z., Wei, Y., & Ye, Q. (2024). Genome-scale CRISPR-Cas9 screening in stem cells: Theories, applications and challenges. *Stem Cell Research & Therapy*, *15*(1), 218. https://doi.org/10.1186/s13287-024-03831-z

Zhu, Y., Huang, S., Chen, S., Chen, J., Wang, Z., Wang, Y., & Zheng, H. (2021). SOX2 promotes chemoresistance, cancer stem cells properties, and epithelial–mesenchymal transition by β-catenin and Beclin1/autophagy signaling in colorectal cancer. *Cell Death & Disease*, *12*(5), 449. https://doi.org/10.1038/s41419-021-03733-5